Final Report

Characterization and Modeling of Photon Absorption on Asphalt Materials for Improved Accuracy and Consistency of Nuclear Density Measurement

Performing Organizations: Columbia University
Manhattan College

August 2015

University Transportation Research Center - Region 2

The Region 2 University Transportation Research Center (UTRC) is one of ten original University Transportation Centers established in 1987 by the U.S. Congress. These Centers were established with the recognition that transportation plays a key role in the nation's economy and the quality of life of its citizens. University faculty members provide a critical link in resolving our national and regional transportation problems while training the professionals who address our transportation systems and their customers on a daily basis.

The UTRC was established in order to support research, education and the transfer of technology in the field of transportation. The theme of the Center is "Planning and Managing Regional Transportation Systems in a Changing World." Presently, under the direction of Dr. Camille Kamga, the UTRC represents USDOT Region II, including New York, New Jersey, Puerto Rico and the U.S. Virgin Islands. Functioning as a consortium of twelve major Universities throughout the region, UTRC is located at the CUNY Institute for Transportation Systems at The City College of New York, the lead institution of the consortium. The Center, through its consortium, an Agency-Industry Council and its Director and Staff, supports research, education, and technology transfer under its theme. UTRC's three main goals are:

Research

The research program objectives are (1) to develop a theme based transportation research program that is responsive to the needs of regional transportation organizations and stakeholders, and (2) to conduct that program in cooperation with the partners. The program includes both studies that are identified with research partners of projects targeted to the theme, and targeted, short-term projects. The program develops competitive proposals, which are evaluated to insure the mostresponsive UTRC team conducts the work. The research program is responsive to the UTRC theme: "Planning and Managing Regional Transportation Systems in a Changing World." The complex transportation system of transit and infrastructure, and the rapidly changing environment impacts the nation's largest city and metropolitan area. The New York/New Jersey Metropolitan has over 19 million people, 600,000 businesses and 9 million workers. The Region's intermodal and multimodal systems must serve all customers and stakeholders within the region and globally.Under the current grant, the new research projects and the ongoing research projects concentrate the program efforts on the categories of Transportation Systems Performance and Information Infrastructure to provide needed services to the New Jersey Department of Transportation, New York City Department of Transportation, New York Metropolitan Transportation Council , New York State Department of Transportation, and the New York State Energy and Research Development Authorityand others, all while enhancing the center's theme.

Education and Workforce Development

The modern professional must combine the technical skills of engineering and planning with knowledge of economics, environmental science, management, finance, and law as well as negotiation skills, psychology and sociology. And, she/he must be computer literate, wired to the web, and knowledgeable about advances in information technology. UTRC's education and training efforts provide a multidisciplinary program of course work and experiential learning to train students and provide advanced training or retraining of practitioners to plan and manage regional transportation systems. UTRC must meet the need to educate the undergraduate and graduate student with a foundation of transportation fundamentals that allows for solving complex problems in a world much more dynamic than even a decade ago. Simultaneously, the demand for continuing education is growing – either because of professional license requirements or because the workplace demands it – and provides the opportunity to combine State of Practice education with tailored ways of delivering content.

Technology Transfer

UTRC's Technology Transfer Program goes beyond what might be considered "traditional" technology transfer activities. Its main objectives are (1) to increase the awareness and level of information concerning transportation issues facing Region 2; (2) to improve the knowledge base and approach to problem solving of the region's transportation workforce, from those operating the systems to those at the most senior level of managing the system; and by doing so, to improve the overall professional capability of the transportation workforce; (3) to stimulate discussion and debate concerning the integration of new technologies into our culture, our work and our transportation systems; (4) to provide the more traditional but extremely important job of disseminating research and project reports, studies, analysis and use of tools to the education, research and practicing community both nationally and internationally; and (5) to provide unbiased information and testimony to decision-makers concerning regional transportation issues consistent with the UTRC theme.

Principal Investigator(s):

Dr. Huiming Yin
Associate Professor
Department of Civil Engineering & Engineering Mechanics
Columbia University
New York, NY 10027
Tel: (212) 851-1648
Email: hy2251@columbia.edu

Dr. Qian Wang
Assistant Professor
Department of Civil and Evironmental Engineering
Manhattan College
Riverdale, NY 10471
Tel: (718) 862-7469
Email: qian.wang@manhattan.edu

Co-author(s):
  -Hoe Ling
  -Wenzheng Feng
  -Fangliang Chen
  -Xin He
  -Liang Wang

1. Report No.	2. Government Accession No.	3. Recipient's Catalog No.

4. Title and Subtitle

Characterization and Modeling of Photon Absorption in Asphalt Materials for Improved Accuracy and Consistency of Nuclear Density Measurement

5. Report Date

August 26, 2015

6. Performing Organization Code

7. Author(s)

Huiming Yin
Qian Wang
Hoe Ling
Wenzheng Feng
Fangliang Chen
Xin He
Liang Wang

8. Performing Organization Report No.

9. Performing Organization Name and Address

Department of Civil Engineering and Engineering Mechanics
Columbia University
500 West 120th Street
New York, NY 100027

10. Work Unit No.

11. Contract or Grant No.
49198-13-26, 49198-14-26

12. Sponsoring Agency Name and Address

UTRC
The City College of New York
137th St. and Convent Avenue
New York, NY 10031

13. Type of Report and Period Covered

14. Sponsoring Agency Code

15. Supplementary Notes

16. Abstract

Although the nuclear density method has been widely used in the compaction measurement of both soils and asphalt pavements, its accuracy for asphalt pavements is not as good as that for soils. Due to this issue, many disputes have incurred in construction projects, which resulted in replacement of the nuclear test method with the core sample method in many state DOTs for quality assurance or acceptance including the DOT Region II states. However, most contractors still use it on quality control as a fast and economic test method. The above disputes can mainly attribute to the effect of asphalt's chemical constitution on the nuclear gauge count readings. There are three basic types of photon interaction with matter, i.e., the Compton, photoelectric, and pair production effects. The Compton effect is dominant in the existing nuclear test methods. Attenuation from the Compton effect is proportional to electron density. Because the hydrogen atom has different ratio of electron/atom mass from other atoms, the content of hydrogen atom in the bulk material may produce significant effects on the nuclear density measurement results. Therefore, to accurately predict material density from the photon count number, the relative composition related to hydrogen needs to be corrected or decoupled.

The goal of this project is to improve the accuracy and consistency of the nuclear test methods in asphalt pavement construction through decoupling the attenuation effect of electrons of hydrogen and other types of atoms. To this end, NIST standard molds with fine aggregate mixed with different contents of foam particles and water as well as asphalt binder have been used for nuclear reading in the direct transmission mode. The hydrogen content (H) has been first measured by neutron scattering. We assume the pure fine aggregate does not contain any hydrogen, which can be used to calibrate the dry density versus the count number. Using the count number (CN) versus actual density (D) at different hydrogen contents, one can obtain the effects of hydrogen atoms and therefore derive the function of CN in term of D and H in the log scale, which exhibits a linear trend approximately as $Ln(CN) = -k_1 D + k_2 H + b$. Our investigation also disclosed that the effect of the mold boundary can be disregarded as long as the source is beyond 4″ to the boundary, but the transmission distance from the source to the detector has significant effect so that the function has different forms for different source depths.

Based on the discovery of this function of CN related to D and H, we can develop a new calibration method of the nuclear gages with ≥3 calibration blocks including one aluminum, one magnesium and one polymer blocks with hydrogen content known. The first two can be used to determine k_1 and b, whereas the last one can be used to determine k_2. Redundant blocks can be used to reduce the accidental errors and improve the accuracy. At the same time, the last two blocks can be used to calibrate the moisture measurement function for neutron scattering. Once the calibration function for a measurement mode is constructed, we can obtain the calibration table for actual measurements.

Because the major improvements are through the fundamental testing principles, the main changes are conducted through the calibration method and count reading analysis. The improved test method will be economically feasible and easy to use as the existing nuclear test method. The team is seeking the opportunity to transfer this technology to industry and demonstrate the method through the field projects. The developed technology together with the new hardware will be released and produce national and international impact on asphalt pavement construction.

.

17. Key Words

Nuclear test method; Density measurement; Moisture effect; Compton Effect; Attenuation Coefficient; Asphalt materials

18. Distribution Statement

(Present in TRB conference)

19. Security Classif (of this report)	20. Security Classif. (of this page)	21. No of Pages	22. Price
Unclassified	Unclassified	60	

Form DOT F 1700.7 (8-69)

Disclaimer
The contents of this report reflect the views of the authors, who are responsible for the facts and the accuracy of the information presented herein. The contents do not necessarily reflect the official views or policies of the UTRC or the Federal Highway Administration. This report does not constitute a standard, specification or regulation. This document is disseminated under the sponsorship of the Department of Transportation, University Transportation Centers Program, in the interest of information exchange. The U.S. Government assumes no liability for the contents or use thereof.

CHARACTERIZATION AND MODELING OF PHOTON ABSORPTION IN ASPHALT MATERIALS FOR IMPROVED ACCURACY AND CONSISTENCY OF NUCLEAR DENSITY MEASUREMENT

EXECUTIVE SUMMARY

Although the nuclear density method has been widely used in the compaction measurement of both soils and asphalt pavements, its accuracy for asphalt pavements is not as good as that for soils. Due to this issue, many disputes have incurred in construction projects, which resulted in replacement of the nuclear test method with the core sample method in many state DOTs for quality assurance or acceptance including the DOT Region II states. However, most contractors still use it on quality control as a fast and economic test method. The above disputes can mainly attribute to the effect of asphalt's chemical constitution on the nuclear gauge count readings. There are three basic types of photon interaction with matter, i.e., the Compton, photoelectric, and pair production effects. The Compton effect is dominant in the existing nuclear test methods. Attenuation from the Compton effect is proportional to electron density. Because the hydrogen atom has different ratio of electron/atom mass from other atoms, the content of hydrogen atom in the bulk material may produce significant effects on the nuclear density measurement results. Therefore, to accurately predict material density from the photon count number, the relative composition related to hydrogen needs to be corrected or decoupled.

The goal of this project is to improve the accuracy and consistency of the nuclear test methods in asphalt pavement construction through decoupling the attenuation effect of electrons of hydrogen and other types of atoms. To this end, NIST standard molds with fine aggregate mixed with different contents of foam particles and water as well as asphalt binder have been used for nuclear reading in the direct transmission mode. The hydrogen content (H) has been first measured by neutron scattering. We assume the pure fine aggregate does not contain any hydrogen, which can be used to calibrate the dry density versus the count number. Using the count number (CN) versus actual density (D) at different hydrogen contents, one can obtain the effects of hydrogen atoms and therefore derive the function of CN in term of D and H in the log scale, which exhibits a linear trend approximately as $Ln(CN) = -k_1 D + k_2 H + b$. Our investigation also disclosed that the effect of the mold boundary can be disregarded as long as the source is beyond $4''$ to the boundary, but the transmission distance from the source to the detector has significant effect so that the function has different forms for different source depths.

Based on the discovery of this function of CN related to D and H, we can develop a new calibration method of the nuclear gages with ≥ 3 calibration blocks including one aluminum, one magnesium and one polymer blocks with hydrogen content known. The first two can be used to determine k_1 and b, whereas the last one can be used to determine k_2. Redundant blocks can be used to reduce the accidental errors and improve the accuracy. At the same time, the last two blocks can be used to calibrate the moisture measurement function for neutron

scattering. Once the calibration function for a measurement mode is constructed, we can obtain the calibration table for actual measurements.

Because the major improvements are through the fundamental testing principles, the main changes are conducted through the calibration method and count reading analysis. The improved test method will be economically feasible and easy to use as the existing nuclear test method. The team is seeking the opportunity to transfer this technology to industry and demonstrate the method through the field projects. The developed technology together with the new hardware will be released and produce national and international impact on asphalt pavement construction.

1. INTRODUCTION

1.1 Research background and problem statement

In the current asphalt pavement construction practice, there are two main approaches to measure the density and compaction of asphalt materials: core sample test and nuclear test. As a more primitive testing method, the core sample test involves extracting core samples and taking them off-site for analysis. The test results are often not available for as long as 24 hours after sampling, which is especially problematic in asphalt construction projects. Moreover, the testing processes are labor-intensive and expensive. On the other hand, as a non-destructive test method, nuclear method uses a portable device, which is placed on the pavement surface, and instantly shows the material density in as short as 1 minute [1,2]. Figure 1 illustrates the field tests using the two methods. For the core sample test, a drill machine shall be transported, some supplies such as water and power source shall be provided as seen in Figure 1(a). After a core sample is extracted and sent to laboratory for density testing, a hole is left in the pavement as seen in Figure 1(b). However, for the nuclear test, the density can be read immediately without any damage to the pavement as seen in Figure 1(c).

Figure 1. Illustrations of core sample test and nuclear test methods: (a) Coring; (b) coring hole, and; (c) nuclear gauge

Nuclear gauges have been world-widely used in the compaction control of pavement construction since Caltrans firstly used it in the 1950s. In its long history, the method has been proved to be safe, precise, and stable for most applications. Especially, it provides excellent accuracy for measuring soil compaction. The nuclear method was originally invented by the petroleum industry for determining densities and liquid quantities in the ground in the later 1940's. The Cornell University first conducted experiments using nuclear methods to determine the subsurface soil moisture and density in 1950. In 1954, Caltrans started to study the nuclear test methods on measuring soil moisture and density in several highway projects

[3]. Some investigation was conducted to improve the test accuracy and formalize the application in highway construction [3–6]. Rapidly, the nuclear test method was adopted by some other states in highway construction quality control [7,8].

The main concern to use the nuclear method in QC/QA project is the considerable difference between the two methods. Surely, the core sample method directly measures the actual density of materials; whereas the nuclear method is an indirect method for electron density. However, what the core sample method measures is not the actual in-field density of asphalt materials. During the coring operation as seen in Figure 1(a), additional densification occurs, and cooling water is forced into the specimen and increases the weight [2]. Moreover, the effect of voids on the surface of cores cannot be excluded, which further increases the measured density compared with the in-field density. In contrast, the nuclear method truly targets at the in-field density of asphalt pavements.

However, some problems do exist within the current nuclear method for the density measurement of asphalt materials. As one member of NGTG formed by California Department of Transportation (Caltrans), the PI Dr. Yin conducted a historical review of Caltrans' pioneer research in the nuclear method, closely communicated with the main nuclear gauge manufacturers, and consulted with Caltrans' researchers and engineers about the usage of nuclear gauges within the state [2]. During this investigation, Dr. Yin identified the main reason that the nuclear method is so successful in soil density measurement, but is disputable in asphalt pavement density measurement. However, some further research and experiments have to be done to address the current problems, to investigate the accuracy and precision of the new test method, and to validate the test method in field construction projects.

In the process of the density measurement with a nuclear gauge, gamma photons are emitted at a specific source, and pass through the test materials. Because photons collide with the electrons of the test material and the probability of the collisions essentially depends on the density of the material, the number of photons that reach the detector can serve as a measurement for the density of the materials: the higher the density of the test materials, the fewer the photons that reach the detectors. Because what a nuclear gauge measures is the number of gamma photons counted by its detector, how to objectively transfer the count into a value of density or moisture is crucially important. Nuclear gauge calibration is to find the correlation between the radiation counts and the density values for the gauge, which can be represented by some curves with specific equations or by a calibration table.

At the early stage, the nuclear gauge calibration data used was either provided by the gauge manufacturer, or generated by field tests. To obtain calibration data from field tests, materials with different densities or compactions were measured by nuclear gauges and another test method [5], and then a correlation between nuclear count readings and actual densities measured by the other test method was established. The calibration curves were generally fitted by linear equations. However, neither of them is satisfactory. The manufacturer ones lack means for references; whereas the field calibrated ones only have a narrow range of field

densities with poor accuracy due to the variability of field test method and non-uniformity of field materials [9]. Engineers turned to develop a permanent laboratory calibration procedure with some standard calibration blocks.

However, the count reading of a nuclear gauge in density measurement is also affected by the chemical constitution of the tested materials, the boundary conditions, the geometry of measurement devices, and energy level of the radioactive source, etc. It is impossible to establish a perfect calibration table of a nuclear gauge for different kinds of materials. As a result, significant differences between the nuclear density reading and the density measured by other test methods may be observed.

Although the nuclear method has been used in the compaction measurement of both soils and asphalt pavements for a long time, its accuracy for asphalt pavements is not as good as that for soils. The correlation of nuclear density results and core densities for asphalt pavements were respectively studied [10–14]. All of these research results showed considerable differences between the nuclear test method and the core sample method. Due to this problem, a lot of disputes incurred in construction projects, and more than half of state DOTs have ceased to use nuclear gauges in the QC/QA projects including all Region II states. Consequently, some new test methods were proposed, such as the vibration based method [15] and the electromagnetic method [16–18], but none of them has the measuring accuracy and stability comparable to the nuclear method, which stimulates us to renovate the existing nuclear density testing and to improve the accuracy of this test method.

In the existing test method, the following steps are conducted:

1. A nuclear gauge is originally calibrated with three metal standard blocks, whose actual densities, at around 110, 135, and 160 pcf, are transferred to soil densities considering the chemical constitution. Based on the nuclear gauge readings and their equivalent soil densities, the calibration constants in a predetermined equation are established and a calibration table is developed. As shown in Figure 2, the calibration curve passes across the calibration points obtained by the three blocks, respectively.

2. To measure density in an asphalt pavement construction project, a test strip of 600 ft long shall be constructed first. Then, both the nuclear density and the core density are obtained. Because the nuclear calibration table aims at soils, the nuclear gauge density reading is surely not accurate, so an offset is observed as seen in Figure 2.

3. During the actual measurement, the density value is obtained through the nuclear gauge density reading plus the offset, which means that the nuclear gauge calibration curve ("Assumed asphalt calibration" curve) for asphalt materials follows the same tendency as soils with a fixed offset.
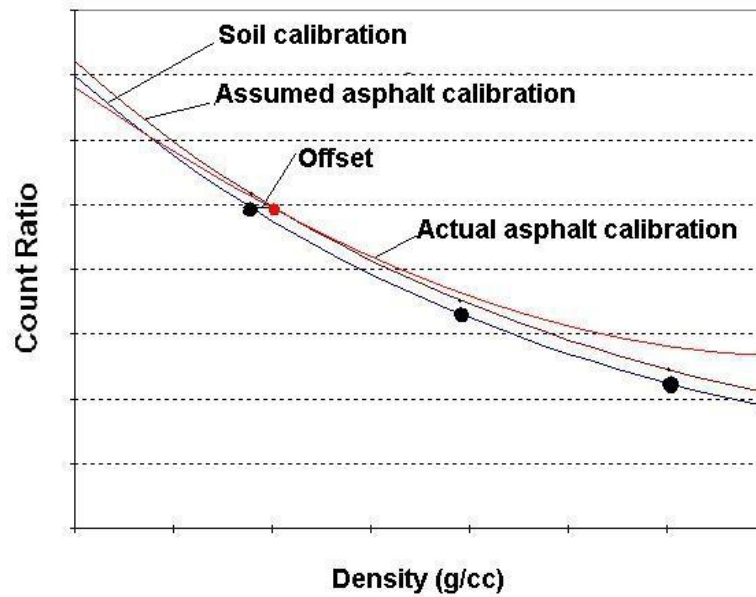
Figure 2. Schematic illustration for the problem in the nuclear gauge.

Because soils and asphalt materials have different chemical constitution, in Figure 2, generally, the asphalt calibration curve follows another tendency, for example, as the red curve marked with "Actual asphalt calibration", which still passes over the red dot with the offset. Obviously, the existing test method cannot obtain the correct density due to the considerable difference between the "Assumed asphalt calibration" curve and the "Actual asphalt calibration" curve. Finding the actual asphalt calibration curve is of the highest priority in this project.

In addition, the existing test method imposes some limitations in the practice. First, to obtain the offset, a test strip with the same job mix formula (JMF) has to been constructed, which means that the existing test method can only be applicable to new construction. If the actual asphalt calibration curve can be obtained, the new test method can be used to measure the density of existing pavement materials. Moreover, during acquiring the offset, the core sample method is used, so the test error of that method is accumulated in the nuclear method. It is crucial to keep the nuclear calibration method independent of the core method in achieving a higher accuracy.

1.2 Research objectives

The proposed work is to investigate the disputable issues in the current test method. The objectives of this study will be addressed through the completion of the following major tasks:

1. Identify the major mechanism to improve the accuracy and consistency of the nuclear measurements
2. Construct the calibration function of nuclear density measurements for pavement materials
3. Develop a new test method and demonstrate the test procedure through preliminary tests

A combined experimental and theoretical approach will be conducted. The proposed project will conduct a thorough literature review about the above research tasks and investigate the fundamental research about the energy absorption difference between asphalt and soil materials, so that the reason why the nuclear method for asphalt materials is not as accurate as that for soils will be quantitatively evaluated. To measure the nuclear gauge count reading changing with asphalt material density, a set of test blocks with different air voids and moisture contents will be prepared. The actual densities of the blocks and nuclear gauge count readings will be measured and analyzed, and an appropriate calibration equation will be developed.

2. LITERATURE REVIEW

A literature review about the problems and concerns of using nuclear gauges in asphalt pavement construction has been conducted. Technical and institutional issues to abandon quality acceptance based on nuclear methods that are perceived by DOTs are also included. This literature review provides some insights and potential solutions for the problems, including the research done at other DOTs and academia, and new development of nuclear gauge technologies. In addition, the count reading of nuclear gauge depending on the material types have been also reviewed.

The nuclear method was originally invented by the petroleum industry for determining densities and liquid quantities in the ground in the later 1940's. Since Cornell University conducted experiments using nuclear methods to determine the subsurface soil moisture and density in 1950, from 1954 to 1958, the California Division of Highways, which was the former of Caltrans, tentatively conducted subsurface measurements of soil moisture and density on several highway projects [19]. Notice that in this report, for consistence, all usages of California Division of Highways are replaced by California Department of Transportation or Caltrans hereafter. By 1958, surface gages have been developed for measuring soil moisture and density. From 1959 to 1961, Caltrans utilized the Nuclear –Chicago surface probes on various highway projects and compared the test results with those by sand volume tests, and found that the densities indicated by the nuclear surface probes could be up to 15 pounds per cubic foot (pcf) higher than the densities determined by sand volume tests. The investigations suggested that the use of a calibration curve for each type of soil would increase the accuracy of the density readings, whereas one moisture calibration was accurate enough for most soils [19]. Therefore, it was proposed to use separate laboratory density calibration curves for different soils to replace the manufacturer density calibration curve for all soils.

With the increase of the knowledge of nuclear test method, in 1964, a standard guide to use nuclear gauge in Caltrans was developed [4], which made it possible for nuclear gauge testing to become a practical test method in quality control of highway construction in California. However, some challenging problems still exist such as how to improve the reproducibility of gauge readings and how to reduce the difference with other test methods. Weber [3] reported the laboratory and field evaluation of nuclear surface gauges for determining soil moisture and density. Eight types of soils from various areas of California were used for laboratory calibration. The use of a density calibration for each soil will significantly increase the accuracy of the readings compared to that using one calibration for all soils. Ten construction projects were investigated by comparing the density readings with the sand volume test and the moisture readings with the oven dry method. An alternative density calibration in field was proposed to calibrate nuclear gauges with a soil under increasing number of passes of a roller. However, the results showed that after four passes, the gauge density readings reach a plateau. Moreover, establishing separate calibration curves for different materials imposed a considerable restriction on the application of nuclear gauges.

In 1964, Caltrans and California Department of Water Resource conducted a cooperative study on nuclear gauge testing [5]. Six different soil types were studies in laboratory including sands, sands and gravel, shale, sandstone, to clay, whose densities had the range from 77 to 148 pcf and whose moistures the range from 3.0 to 27.5 pcf. For each test mode of density calibrations, all the soil samples were used, which was different from the previous proposed procedure using separate calibration for each type of soil [3]. Two types of linear density calibration functions were investigated for the backscatter mode. Both functions exhibit the similar performance with slight differences. This study also demonstrated that collimation of the emission source could considerably reduce the standard deviation of the calibration data compared with the experimental results in the backscatter mode. It was noted that some visual fitted curves were closer to the experimental results than the straight lines. Unfortunately, no effort was conducted to seek a better calibration function. Obviously, if a poor calibration function is chosen, it does not make sense to evaluate the experiments based on the standard deviation of the test data from the fitting curve.

With the major deficiencies being overcome, Caltrans practiced using nuclear density and moisture gauge in actual construction projects for compaction control. In 1964-1965, a two-phase field program was undertaken. In the first phase, nuclear tests were conducted by one operator using one nuclear soil gauge in five construction projects located in Caltrans Districts 03 and 10 [20]. In parallel, sand volume tests were also performed at the same location on the ground where the nuclear gauge had been placed. Using the sand volume test results and nuclear gauge readings, calibration curves were generated with the linear regression method. However, the standard deviation ranged from 5 to 10 pcf [20]. Therefore, a method of "multiple testing" was proposed to use the average density in compaction control. The second phase involved the actual specification of nuclear control testing in the contract special provisions for replacing the sand volume tests. The project proved that nuclear test method was ideally suited for a wide variety of conditions and materials [5]. Therefore, Caltrans officially started to use nuclear gauges in compaction control in 1966.

From 1966 to 1968, Caltrans extensively investigated the test method using nuclear gauge to control soil compaction in the whole state [6,21–25]. The direct transmission type nuclear gauges provided an excellent performance with the accuracy comparable to the sand volume test. It recommended using a single density calibration curve for all soils for deeper probe positions. Field calibration by correlation with in-place densities determined by the sand volume method was discouraged, whereas the laboratory calibration with some standard blocks was recommended, especially for the direct transmission mode. When widely using nuclear gauge in soil compaction control, Caltrans also initiated research on the nuclear test method for asphalt pavement compaction control [26]. The major challenge considered was the effect of temperature, which could change the radiation readings and affect the workability of gauges.

Although the calibration curves of a nuclear gauge could be obtained from the gage manufacturer or generated by the field test, neither of them is satisfactory, because the

manufacturer ones are lack of means for references, whereas the field calibrated ones only have a narrow range of field densities with poor accuracy due to the variability of field test method and non-uniformity of field materials. To develop a permanent laboratory calibration procedure, a comprehensive research project titled "Calibration Standards for Nuclear Gauges" was launched in 1968 [9,27]. A set of six master density gage calibration standard blocks was established. The set, three calcareous and three siliceous standard blocks, represents the predominant mineralogy of California highway soils. Three of the six blocks were cut from nature stone and the remainders cast of Portland cement and selected aggregates. A set of two moisture standard blocks was also fabricated of silica sand, one of which was kept dry in a sealed container and the other was fully saturated with water. A detailed calibration procedure was developed as seen in California Test Method 911 (CTM 911) [28], which was later changed to CTM 111[29].

During the density calibration, a straight line on the semi-logarithmic coordinate as Eq. (1) was used, so that only two calibration constants were needed. However, the plot of calibrations showed that the relation of densities to count ratios is slightly curvilinear [9], so that the relation is approximated by two segments of straight lines with slightly different slopes meeting at 130-135 pcf, which would obviously need four calibration constants. In addition, an inflexion point exists at the joint of the two segments, which has no physical explanation.

The moisture calibration used a straight line to approximate the relation of moisture contents to count ratios. Four types of soils were tested, and research results showed that the lines had very similar slope for all types of soils. The difference between lines might be from the effects of the structural water and absorbing elements [27].

Since then, the major efforts of Caltrans were to improve the performance of nuclear gauge and to extend the applications of nuclear gauge [10,30–34]. However, the nuclear gauge calibration procedure did not change until Zha introduced a procedure for density calibration using a set of three metal standard blocks[35], which results in substantial revisions of the CTM111. However, the linear regression equation (1) was still adopted, and the calibration data of the three metal blocks should still be correlated to those from the six master blocks. The equivalent soil densities for the metal blocks were established based on a great amount of calibration data conducted by 33 nuclear gauges, and a specific acceptable deviation limit and a correlation coefficient limit are introduced to control the repeatability of gauge reading and the precision of calibration. However, in the implementation of CTM 111, some major problems have been found as follows:

1. After being used for so many years, the six mater density standard blocks have become not stable and changed their densities from year to year [35] and the water tubs in moisture calibration have corroded.

2. The linear regression method for density calibration imposes a correlation coefficient limit 0.999 for each calibration curve, which causes a great number of nuclear gauges being recalibrated or failed in calibration.

3. With the appearance of Direct Readout capabilities for most new gauges, because the previous Caltrans calibration procedure is not compatible with the built-in algorithm, Caltrans testers cannot utilize this function, so that they have difficulties to communicate with colleagues from other states.

3. BASIC PHYSICS OF RADIATION

3.1 Radiation

Radiation is energy in the form of waves of particles. There are two forms of radiation: nonionizing and ionizing radiations. Non-ionizing radiation has less energy than ionizing radiation; it does not possess enough energy to produce ions. Examples of non-ionizing

radiation are visible light, infrared, radio waves, microwaves, and sunlight. Ionizing radiation is capable of knocking electrons out of their orbits around atoms, upsetting the electron/proton balance and giving the atom a positive charge. Electrically charged molecules and atoms are called ions.

There are several types of ionizing radiation: Alpha radiation (α), Beta radiation (β), Photon radiation (gamma [γ] and X-ray), and Neutron radiation. Alpha radiation consists of alpha particles that are made up of two protons and two neutrons each and that carry a double positive charge. Due to their relatively large mass and charge, they have an extremely limited ability to penetrate matter. Alpha radiation can be stopped by a piece of paper or the dead outer layer of the skin. Beta radiation consists of charged particles that are ejected from an atom's nucleus and that are physically identical to electrons. Beta particles generally have a negative charge, are very small and can penetrate more deeply than alpha particles. However, most beta radiation can be stopped by small amounts of shielding, such as sheets of plastic, glass or metal. Photon radiation is electromagnetic radiation. [Introduction-to Radiation-eng].

Gamma [γ] and X-ray are often referred to as photon radiations. Gamma radiation consists of photons that originate from within the nucleus, and X-ray radiation consists of photons that originate from outside the nucleus, and are typically lower in energy than gamma radiation. As none of them has charges, they do not directly apply impulses to orbital electrons as alpha and beta particles do. Photon radiation proceeds through matter until there is a chance of interaction with a particle. If the particle is an electron, it may receive enough energy to be ionized, whereupon it causes further ionization by direct interactions with other electrons. Thus, photon radiation can penetrate very deeply and sometimes can only be reduced in intensity by materials that are quite dense, such as lead or steel. Because these neutral radiations undergo only chance encounters with matter, they do not have finite ranges, but rather are attenuated in an exponential manner. In other words, a given gamma ray has a definite probability of passing through any medium of any depth.

Neutron is a subatomic particle with no net electric charge and a mass slightly larger than that of a proton. Protons and neutrons, each with mass approximately one atomic mass unit, constitute the nucleus of an atom. Neutrons lose energy in matter by collisions which transfer kinetic energy. This process is called moderation and is most effective if the matter the neutrons collide with has about the same mass as the neutron. Once slowed down to the same average energy as the matter being interacted with (thermal energies), the neutrons have a much greater chance of interacting with a nucleus. Such interactions can result in material becoming radioactive or can cause radiation to be given off. Apart from cosmic radiation, spontaneous fission is the only natural source of neutrons (n). A common source of neutrons is the nuclear reactor, in which the splitting of a uranium or plutonium nucleus is accompanied by the emission of neutrons. The neutrons emitted from one fission event can strike the nucleus of an adjacent atom and cause another fission event, inducing a chain reaction [36,37].

3.2 Interaction of radiation with matter

When photon radiations are directed into an object, some of the photons interact with the particles of the matter and their energy can be absorbed or scattered. This absorption and scattering is called attenuation. The number of photons transmitted through a material depends on the thickness, density and atomic number of the material, and the energy of the individual photons. Even when they have the same energy, photons travel different distances within a material simply based on the probability of their encounter with one or more of the particles of the matter and the type of encounter that occurs. Since the probability of an encounter increases with the distance travelled, the number of photons reaching a specific point within the matter decreases exponentially with distance travelled which is illustrated in Figure 3.
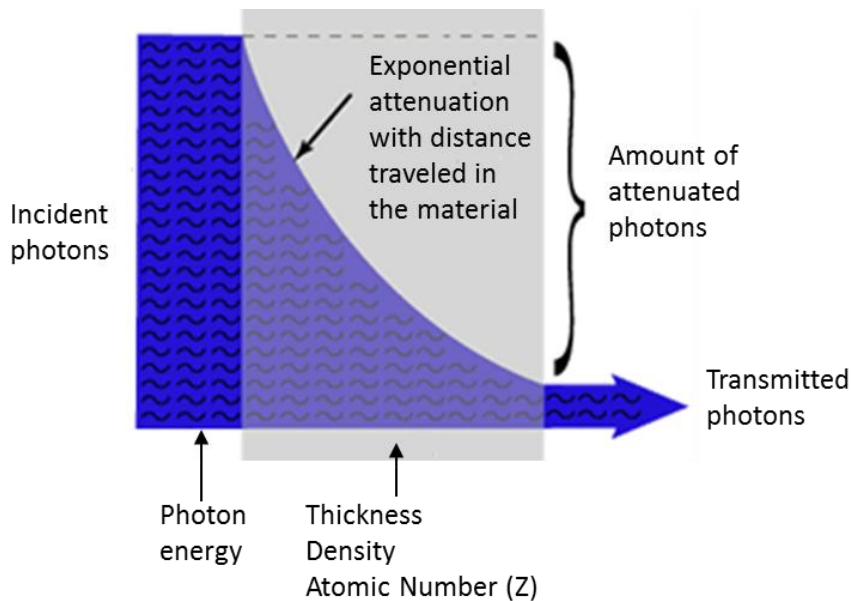

Figure 3. Illustration of photons transmitting through a material.

The formula that describes this curve is:

$$I = I_0 e^{-\mu x} \tag{1}$$

where *I* is the intensity of photons transmitted across some distance *x, I_0* is the initial intensity of photons, μ is the linear attenuation coefficient, and x is the travelled distance.

The linear attenuation coefficient (μ) describes the fraction of a beam of photon radiation that is absorbed or scattered per unit thickness of the absorber. This value basically accounts for the number of atoms in a cubic cm volume of material and the probability of a photon being scattered or absorbed from the nucleus or an electron of one of these atoms.

Since a linear attenuation coefficient is dependent on the density of a material, the mass attenuation coefficient is often reported for convenience. Normalizing μ by dividing it by the density of the element or compound will produce a value that is constant for a particular

element or compound. This constant ($\mu_m = \frac{\mu}{\rho}$) is known as the mass attenuation coefficient and has units of cm^2/gm.

To convert a mass attenuation coefficient (μ_m) to a linear attenuation coefficient (μ), simply multiply it by the density (ρ) of the material.

$$\mu = \mu_m \rho \qquad \qquad (2)$$

The attenuation that results due to the interaction between penetrating radiation and matter is not a simple process. A single interaction event between a primary x-ray photon and a particle of matter does not usually result in the photon changing to some other form of energy and effectively disappearing. Several interaction events are usually involved and the total attenuation is the sum of the attenuation due to different types of interactions. These interactions include the photoelectric effect, scattering, and pair production. shows an approximation of the total absorption coefficient (μ), in red, for iron plotted as a function of radiation energy. The four radiation-matter interactions that contribute to the total absorption are shown in black. The four types of interactions are: photoelectric (PE), Compton scattering (C), pair production (PP), and Thomson or Rayleigh scattering (R). Since most industrial radiography is done in the 0.1 to 1.5 MeV range, it can be seen from the plot that photoelectric and Compton scattering account for the majority of attenuation encountered.

Photoelectric (PE) absorption occurs when the photon is absorbed, resulting in the ejection of electrons from the outer shell of the atom, and hence the ionization of the atom. Subsequently, the ionized atom returns to the neutral state with the emission of an x-ray characteristic of the atom. This subsequent emission of lower energy photons is generally absorbed and does not contribute to (or hinder) the image making process. Photoelectron absorption is the dominant process for x-ray absorption up to energies of about 500 KeV. Photoelectron absorption is also dominant for atoms of high atomic numbers.

Compton scattering (C) occurs when the incident photon is deflected from its original path by an interaction with an electron. The electron gains energy and is ejected from its orbital position. The photon loses energy due to the interaction but continues to travel through the material along an altered path. Since the scattered photon has less energy, it, therefore, has a longer wavelength than the incident photon. The event is also known as incoherent scattering because the photon energy change resulting from an interaction is not always orderly and consistent. The energy shift depends on the angle of scattering and not on the nature of the scattering medium.
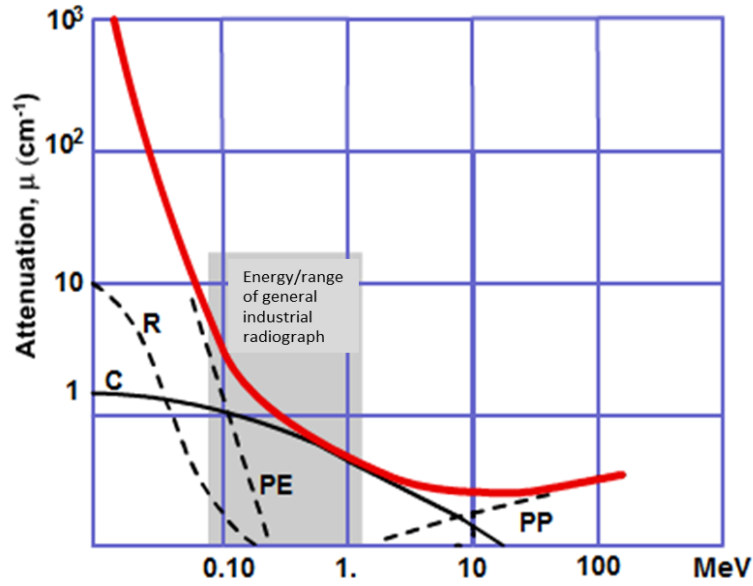
Figure 4. Summary of different mechanisms that cause attenuation of an incident photon beam[38].

Pair production (PP) can occur when the photon energy is greater than 1.02 MeV, but really only becomes significant at energies around 10 MeV. Pair production occurs when an electron and positron are created with the annihilation of the photon. Positrons are very short lived and disappear (positron annihilation) with the formation of two photons of 0.51 MeV energy. Pair production is of particular importance when high-energy photons pass through materials of a high atomic number.

Thomson scattering (R), also known as Rayleigh, coherent, or classical scattering, occurs when the photon interacts with the whole atom so that the photon is scattered with no change in internal energy to the scattering atom, nor to the photon. In this scattering, photons are scattered by bound electrons in a process in which the scattering atom is neither excited nor ionized. Since coherent scatter is only important at high values of Z and for energies of a few KeV, Thomson scattering is never more than a minor contributor to the absorption coefficient. The scattering occurs without the loss of energy and is mainly in the forward direction.

3.3 Attenuation coefficient

As mentioned previously, the total attenuation is the sum of the attenuation due to different types of interactions. Compton scattering is the interaction of the photon with a quasi-free charged particle, usually an electron. It results in a decrease of energy of the photon which is called Compton effect. The decrease of photon intensity can be calculated as:

$$I = I_0 e^{-\mu_m \rho x} \tag{3}$$

where I_0 is the initial intensity of incident photon, I is the intensity of photon detected at the detector, μ_m is called mass attenuation coefficient caused by Compton effect, ρ is the

density of the test material, x is the distance that the photon transmits through the test material. For the mass attenuation coefficient of test material which contain only one kind of atoms, it can be written as:

$$\mu_m = C(\lambda)\frac{Z}{A} \tag{4}$$

$C(\lambda)$ is a function of the wave length of incident photon, Z and A is the atomic number and molar mass of the test material, respectively. For hydrogen $\frac{Z}{A}$ is equal to 1, however for other atoms, it is 0.5. For material which is formed by differnt atom, the mass attenuation coefficient is:

$$\mu_m = \sum_i \eta_i (\mu_m)_i \tag{5}$$

η_i is the mass ratio of the ith atom, $(\mu_m)_i$ is the mass attenuation coefficient of the ith atom.

4. THEORETICAL MODEL

In this part, we apply a simple model shown in Figure 5 to illustrate how the moisture content affects the density reading. As shown in Figure 5, the photon emitted from the source with initial intensity I_0 transmit directly through the test material, then the intensity of photon detected at the right side by the detector is I. Then according to the principle of Compton effect introduced in part 2, we can get the relationship between I and I_0:

$$I = I_0 e^{-\mu_m \rho L} \tag{6}$$

Based on Eq. (3), and that the mass attenuation coefficient of hydrogen is $C(\lambda)$ while it is $0.5C(\lambda)$ for other atoms, then we can write μ_m as:

$$\mu_m = C(\lambda)(\eta_H + 0.5\eta_{others}) \tag{7}$$

η_H and η_{others} are the mass ratio of hydrogen and other atoms, respectively.
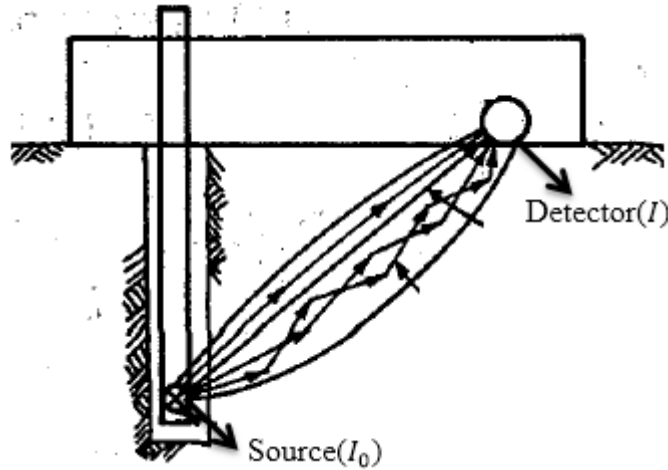

Figure 5 Illustration of photon source transmitting and scattering in a material.

The hydrogen appears in the form of water or moisture in the material mainly, so under the assumption that except water in the material, hydrogen does not exist in other forms, therefore we can set up the relationship between μ_m and moisture M as follows, here we use the same dimension for moisture with density (pcf), v is the volume of test marterial.

$$\eta_{others} + \eta_H = 1 \tag{8}$$

So, substitute Eq. (8) into Eq. (7), we can rewritten Eq. (7) as:

$$\mu_m = \frac{C(\lambda)}{2}(1 + \eta_H) \tag{9}$$

The mass of hydrogen can be written as:

$$m_H = v \cdot M \cdot \frac{2}{18} = \frac{Mv}{9} \tag{10}$$

Then the mass ratio of hydrogen is:

$$\eta_H = \frac{m_H}{m_{total}} = \frac{\frac{Mv}{9}}{\rho v} = \frac{M}{9\rho} \tag{11}$$

Based on Eq. (11), Eq. (9) changes to:

$$\mu_m = \frac{C(\lambda)}{2}\left(1 + \frac{M}{9\rho}\right) \tag{12}$$

Then using Eq. (12) and (6), we can get the relationship between I, I_0 and M as:

$$ln\frac{I}{I_0} = -\frac{(\rho+\frac{M}{9})LC(\lambda)}{2} \tag{13}$$

According to the principle of nuclear gage, it tests the density based on the change of photon intensity, so, from Eq. (13), for material with moisture, the test result is $\rho + \frac{M}{9}$, which is the sum of test material density and one ninth of moisture. That means that, in order to get density calibration curve of material with moisture, we need to shift the calibration curve for dry material by one ninth of moisture.

Specifically, for material where hydrogen does not exist as form of moisture, such as asphalt, we need use the mass ratio of hydrogen in this material to investigate the effect of hydrogen to the density reading separately.

Substitute Eq. (9) to Eq. (6), yields:

$$ln\frac{I}{I_0} = -\frac{(\rho+\rho\,\eta_H)LC(\lambda)}{2} \tag{14}$$

Therefore, using the count number got from the testing of this kind of material, hydrogen does not exist as form of water, we can get a density based on the density calibration curve used for the material without water or hydrogen. Then dividing this density by $1 + \eta_H$, we can get the real density for this hydrogen included material.

5. EXPERIMENTAL VALIDATION.

5.1 Mixing design and sample preparation

To investigate the energy absorption difference for gamma rays among asphalt and sand mixed with different foam particles at different moisture contents, totally 26 tanks of samples were prepared by the NIST standard size moulds ($24'' \times 17'' \times 12''$). For each test, the nuclear source was placed through a pre-prepared hole (either pre-drilled for sand material or preinstalled via a PVC tube for asphalt binder) located at $4''$ (or $6''$) from its closed end and $8.5''$ from the two edges. A schematic illustration is shown in Figure 6. During the test, the Geiger counter detector which is embedded in the nuclear gauge device will be placed $10''$ away from the source rod on the sample surface to count the detected photons for 1 minute.
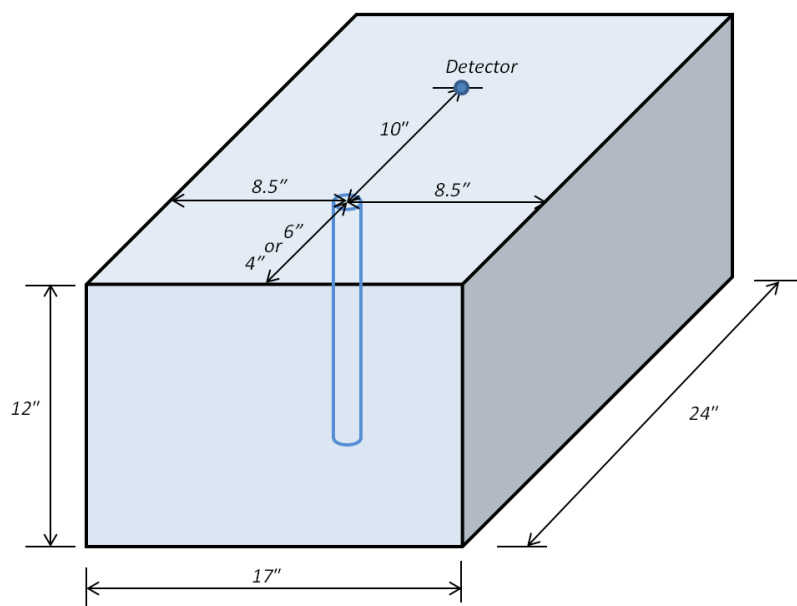

Figure 6. NIST standard size moulds with PVC tube inside.

5.1.1 Mixed sand with different foam particles and different moisture contents

Dry fine natural screened and washed sand (Figure 7 (a)) bought from local Home depot were used to mix the foamed polymer particles (Figure 7 (b)) with different moisture contents. The density of the sand ranges from 1504.1kg/ m^3 to 1661.5 kg/ m^3 for loose and compacted one, respectively. The foamed polymer particles shown in Figure 7 (b) is the Elemix Type XE Concrete Additive provided by NOVA Chemicals Inc. The maximum sphere diameter is 0.25 inch (6.4 mm), bulk density is 1.10 lb/ft^3 (17.6 kg/m^3) and specific gravity is 0.0176.

Five different foam particle volume fractions (0, 4%, 8%, 12%, 16% and 20%) and five different moisture contents (2, 4, 6, 8, 10 pcf) were prepared. Our preliminary test showed that the dry sand can't be mixed well with foam particles due to its extreme light weight. The mix design of the sand with different foam particles and moisture content is shown in Table 1. The gravity for each sample block can be calculated by measuring the weight of the total material introduced into the mould and its compacted volume.

Figure 7. (a) Natural screened and washed sand; and (b) Foamed polymer particles

Table 1 Mixing design of sand with different amount of foam particle and moisture contents

Foam volume fraction	Added components	Moisture content				
		2%	4%	6%	8%	10%
4%	Sand (lbs)	219.3	219.3	219.3	219.3	219.3
	Foam (L)	2.674	2.674	2.674	2.674	2.674
	Water (lbs)	4.72	9.44	14.17	18.89	23.61
	Density (lbs/ft3)	95.00	97.00	99.00	101.00	103.00
8%	Sand (lbs)	210.19	210.19	210.19	210.19	210.19

	Foam (L)	5.348	5.348	5.348	5.348	5.348
	Water (lbs)	4.72	9.44	14.17	18.89	23.61
	Density (lbs/ft3)	91.26	93.26	95.26	97.26	99.26
12%	Sand (lbs)	201.06	201.06	201.06	201.06	201.06
	Foam (L)	8.023	8.023	8.023	8.023	8.023
	Water (lbs)	4.72	9.44	14.17	18.89	23.61
	Density (lbs/ft3)	87.51	89.51	91.51	93.51	95.51
16%	Sand (lbs)	192.02	192.02	192.02	192.02	192.02
	Foam (L)	10.697	10.697	10.697	10.697	10.697
	Water (lbs)	4.72	9.44	14.17	18.89	23.61
	Density (lbs/ft3)	83.80	85.80	87.80	89.80	91.80
20%	Sand (lbs)	182.76	182.76	182.76	182.76	182.76
	Foam (L)	13.371	13.371	13.371	13.371	13.371
	Water (lbs)	4.72	9.44	14.17	18.89	23.61
	Density (lbs/ft3)	80.00	82.00	84.00	86.00	88.00

The Kushlan Products 350 Direct Drive Mixer was used to mix the particulate composites. The 3.5 cu. ft. capacity drum holds up to 180 lbs. premixed composite and the ¾ HP electric motor provides 28 rotations per minute. Considering the sample volume to be filled in the mould, we divided the material into two parts and mix them separately. The mixing and sample preparation procedures are provided as follows (Figure 8):

Figure 8 Sample mixing and preparation

1. Weight half mass of sand and volume of polymer provided in Table 1 into the mixer.
2. Add half of water of each part into the mixer, then turn on the mixer to make the container turn half circle and stop the mixer.
3. Introduce the left water into the mixer.
4. Turn on the mixer to mix the polymer, sand and water for five minutes. During the mixing process, a plastic hammer was used to knock the drum frequently to prevent the material from sticking to the mixer drum boundary.
5. After mixing, pour the material in to the mould.
6. Compact the mixed composites to the predetermined volume, which is controlled by two lines which were marked at a distance of 7 inches and 2 inches respectively to the top edge of the mould. The surface of the prepared sample at its completion stage remains a flat one. Figure 9 shows prepared composite sample with mixed sand and foaming particle.

Figure 9. A prepared composite sample with mixed sand and foaming particles.

5.1.2 Asphalt binder

The Asphalt Cement with sample grade of PG 64-22 supplied from the Axeon Specialty Products, LLC was used in this study. The material properties of the selected Asphalt binder provided by the manufacture are summarized in Table 2.

Table 2 Material properties of Asphalt binder

Method	Test	Result	units	Spec Limit
AASHTO T228	Specific Gravity @ 77ºF	1.087		
AASHTO T48	Flash Point	289	ºC	Min 230
AASHTO T316	Viscosity @135 ºC	0.461	Pa.s	Max 3.0
	Viscosity @165 ºC	0.125	Pa.s	Report
AASHTO T315	ODSR test temperature	64	ºC	
AASHTO T313	Creep Stiffness @ 60 sec	144	MPa	Max 300

For the asphalt binder test, as the nuclear source, which is located in an extendable rod embedded in the nuclear gauge, needs to be inserted to different depth of the test samples. Two plastic tubes with the same diameter of the nuclear source rod were pre-mounted at the bottom of the mould (as shown in Figure 10 (a)). Four barrels of asphalt binder with 75 lbs per each were heated to 120 ºC and then pour into the mould which is shown in shown in Figure 10 (b). The filling height of the asphalt binder in the mould is 9 inches.
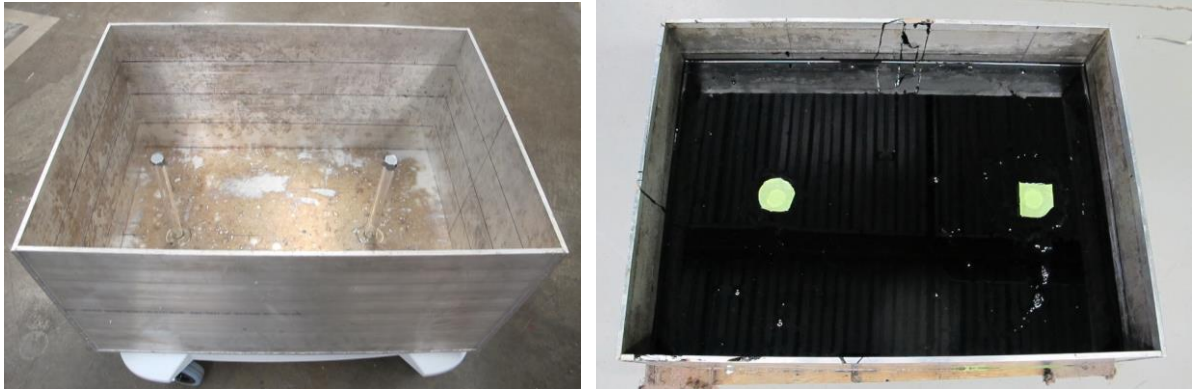
Figure 10. Asphalt sample preparations.

5.2 Laboratory testing

In order to decouple the effects of photon and neutron sources on the count reading, two customized nuclear gauges were fabricated by the Troxler Electronic Laboratories. To measure the sample density, the Troxler Model 3430 plus was used by taking away the original neutron radiation source as shown in Figure 11(a). In the direct transmission position (with the source rod extend into the material to be measured), the source rod extends through the base of the gauge into a pre-drilled hole to a desired depth (4″, 6″, and 8″). Photons from the cesium-137 (Cs-137) source in the source rod pass through the test material. While passing through the test material, the photons collide with electrons and lose energy. A high material density increases the probability of those photon collisions. This decreases the number of photons that reach the Geiger-Muller (G-M) detectors in the base of the gauge. Thus, the number of photons reaching the detectors is inverse related to the density of the material: the higher the density of the material, the fewer the photons that reach the detectors.

While for moisture measurement, the gauge uses the principle of neutron thermalization to monitor the moisture content of a material. The gauge includes an americium-241: beryllium (Am-241:Be) source that is fixed in the gauge's base (Figure 11(b)). Fast neutrons emitted by the Am-241:Be source pass into the test material. Multiple collisions between the fast neutrons and a similarly sized mass (such as the nuclei of hydrogen atoms) cause the neutrons to slow to the point where further collisions with hydrogen or other materials will not continue to reduce the neutron energy further. The neutrons are said to have been thermalized. The gauge contains a helium-3 detector that is sensitive only to thermalized, or slow neutrons. As a result, the moisture counts relate directly to the amount of hydrogen in the material.

Figure 11. Nuclear gauge devices: (a) Cs-137 source; and (b) Am-241: Be source.

A scraper plate was used to further smoothen the compacted sample surface and prepare the pre-drilled holes for the source rod to reach to a desired depth. The dimensions of the scraper plate match the base of the gauge that they are paired with. This is a safety feature that, once the hole has been drilled, a template for the base of the gauge has been created. By simply etching around the base of the scraper plate before picking it up, the gauge can be easily placed down inside of this etched area and the opening for the source rod will be positioned over the hole pre-drilled. By using this method one will be able to use the gauge without ever visually seeing the source rod, which will ensure that the exposure to gauge radiation will be minimized. For each sample, two pre-drilled holes were prepared, one is located at 4 inches near to its adjacent end and another is 6 inches, to investigate the potential boundary effects (Figure 9). Before taking a test the gauge was pushed towards the side of the hole with the detector tubes to ensure that there is no air gap between the source rod and the side of the hole. During the measurement, the count time for both radiation sources was set to 1 minute, which defines how long the gauge reads. In general, a longer count time produces better measurement precision. Troxler recommends a count time of 1 minute for most sample measurements.

For the asphalt binder, as the nuclear gauge device (about 20 lbs) is placed on the binder surface for certain period (few minutes), which requires that the sample surface to maintain in a flat plane. However as the binder is viscoelastic, it is not able to sustain the test gauge for that long period. Therefore, two steel bars were shaped and positioned onto the mould to support the nuclear gage as shown in Figure 12 (a). A plastic film was further placed on the top surface of the asphalt binder to avoid any contamination left on the bottom surface of the nuclear gauge.

Figure 12. Asphalt sample testing

5.3 Test results and interpretations:

Totally 12 count readings were recorded for each compacted sample (2 radiation sources × 3 depths × 2 boundaries). The recorded count numbers are shown in Tables 3 - 8. Because of the unavailable neutron device during the test, the neutron count number for the sample with 4% foaming polymer at 2 pcf moisture content was not recorded.

Table 3 Nuclear gage reading result for tested material with 4% foaming polymer.

Moisture (pcf)	Distance to Boundary	Source type	Depth of source		
			4 inches	6 inches	8 inches
2	4 ″	Cs-137	93536	77664	56384
		Am-241:Be	-	-	-
	6″	Cs-137	94496	78400	56288
		Am-241:Be	-	-	-
4	4 ″	Cs-137	94240	78496	54688
		Am-241:Be	560	624	720
	6″	Cs-137	93776	78768	55744
		Am-241:Be	672	800	848
6	4 ″	Cs-137	91376	75840	52320
		Am-241:Be	816	1040	1072
	6″	Cs-137	93264	77344	54192
		Am-241:Be	960	1120	1312
8	4 ″	Cs-137	89280	72288	51312
		Am-241:Be	1168	1424	1568
	6″	Cs-137	89232	72256	50032
		Am-241:Be	1312	1504	1728
10	4 ″	Cs-137	88560	70896	48640
		Am-241:Be	1520	1776	1904
	6″	Cs-137	87952	70960	48512
		Am-241:Be	1680	1936	2064

Table 4 Nuclear gage reading result for tested material with 8% foaming polymer.

Moisture (pcf)	Distance to Boundary	Source type	Depth of source		
			4 inches	6 inches	8 inches
2	4 ″	Cs-137	100256	83920	60048
		Am-241:Be	304	384	448
	6″	Cs-137	101168	84960	60656
		Am-241:Be	352	400	480
4	4 ″	Cs-137	97536	81920	59008
		Am-241:Be	576	720	768
	6″	Cs-137	98848	82944	58928
		Am-241:Be	704	752	880
6	4 ″	Cs-137	96560	79184	56784
		Am-241:Be	880	1072	1200
	6″	Cs-137	97712	81056	56640
		Am-241:Be	928	1088	1216
8	4 ″	Cs-137	96160	79536	56304
		Am-241:Be	1152	1376	1536
	6″	Cs-137	97168	79808	55376
		Am-241:Be	1200	1376	1600
10	4 ″	Cs-137	95360	77008	51648
		Am-241:Be	1520	1824	2016
	6″	Cs-137	95536	77216	52480
		Am-241:Be	1584	2032	2208

Table 5 Nuclear gage reading result for tested material with 12% foaming polymer.

Moisture (pcf)	Distance to Boundary	Source type	Depth of source		
			4 inches	6 inches	8 inches
2	4 ″	Cs-137	106496	90768	66048
		Am-241:Be	336	400	464
	6″	Cs-137	107344	90816	66048
		Am-241:Be	352	432	512
4	4 ″	Cs-137	104656	90368	63856
		Am-241:Be	640	720	928
	6″	Cs-137	105504	88768	64544
		Am-241:Be	704	864	912
6	4 ″	Cs-137	104912	88992	63392
		Am-241:Be	800	992	1168
	6″	Cs-137	104544	87968	62656

		Am-241:Be	928	1120	1248
8	4 ″	Cs-137	103008	85904	60608
		Am-241:Be	1184	1376	1600
	6″	Cs-137	103856	86592	61776
		Am-241:Be	1216	1552	1808
10	4 ″	Cs-137	102368	83728	57056
		Am-241:Be	1360	1712	1904
	6″	Cs-137	102336	84032	57248
		Am-241:Be	1504	1776	2064

Table 6 Nuclear gage reading result for tested material with 16% foaming polymer.

Moisture (pcf)	Distance to Boundary	Source type	Depth of source		
			4 inches	6 inches	8 inches
2	4 ″	Cs-137	115984	99792	73216
		Am-241:Be	304	352	384
	6″	Cs-137	115696	100160	73680
		Am-241:Be	352	400	416
4	4 ″	Cs-137	112160	94560	70416
		Am-241:Be	608	704	752
	6″	Cs-137	111936	95408	70160
		Am-241:Be	704	720	848
6	4 ″	Cs-137	110768	92368	67696
		Am-241:Be	880	1056	1232
	6″	Cs-137	111792	94080	67440
		Am-241:Be	976	1120	1248
8	4 ″	Cs-137	108768	91104	63936
		Am-241:Be	1104	1408	1488
	6″	Cs-137	109056	91328	65632
		Am-241:Be	1232	1584	1744
10	4 ″	Cs-137	105280	86560	60688
		Am-241:Be	1552	1872	2000
	6″	Cs-137	107168	90288	61792
		Am-241:Be	1632	2016	2128

Table 7 Nuclear gauge reading result for tested material with 20% foaming polymer.

Moisture (pcf)	Distance to Boundary	Source type	Depth of source		
			4 inches	6 inches	8 inches
2	4 ″	Cs-137	119168	103664	77760
		Am-241:Be	336	304	336

	6″	Cs-137	120048	103296	77536
		Am-241:Be	352	432	512
4	4 ″	Cs-137	115312	98912	73216
		Am-241:Be	624	752	736
	6″	Cs-137	114784	99456	73600
		Am-241:Be	704	848	896
6	4 ″	Cs-137	112544	96896	72592
		Am-241:Be	784	944	1056
	6″	Cs-137	113184	96816	72432
		Am-241:Be	1008	1136	1232
8	4 ″	Cs-137	110048	93360	68512
		Am-241:Be	1152	1360	1632
	6″	Cs-137	111008	93136	68048
		Am-241:Be	1296	1552	1696
10	4 ″	Cs-137	110160	90496	63344
		Am-241:Be	1632	2000	2160
	6″	Cs-137	111136	91056	63776
		Am-241:Be	1824	2080	2256

Table 8 Nuclear gauge reading result for asphalt binder.

Distance to Boundary	Source type	Depth of source		
		4″	6″	8″
4″	Cs-137	143504	128832	100592
	Am-241:Be	1104	2320	4096
6″	Cs-137	142528	130560	101936
	Am-241:Be	1088	2336	4160

The variances of the counting readings with respect to different polymer volume fractions at different boundaries are shown in **Error! Reference source not found.** to **Error! Reference source not found.**.   **Error! Reference source not found.** and **Error! Reference source not found.** show that the photon count number gradually increase as the polymer volume fraction increases.   Notes that for these samples with the same predetermined volume, the density of the mixed sample continually decreases as the polymer volume fraction increases. Thus, **Error! Reference source not found.** and **Error! Reference source not found.** indicates that the photon count number gradually increase as their density decrease. For the neutron readings, **Error! Reference source not found.** and **Error! Reference source not found.** show that, excluding the test errors, the neutron count number almost keep constant with respect to the

polymer content. It indicates that the neutron number is independent on the sample density when the moisture contents in the sample are the same. It seems from **Error! Reference source not found.** to **Error! Reference source not found.** that the boundary effects (different distances from the radiation sources to the boundary) on both the photon and neutron readings are negligible.

Photon reading V.S. Polymer
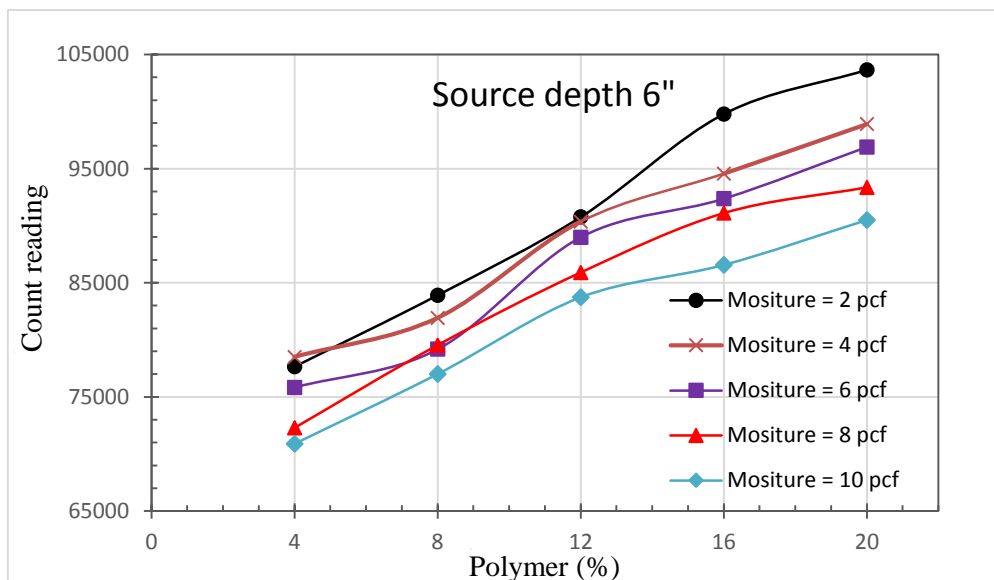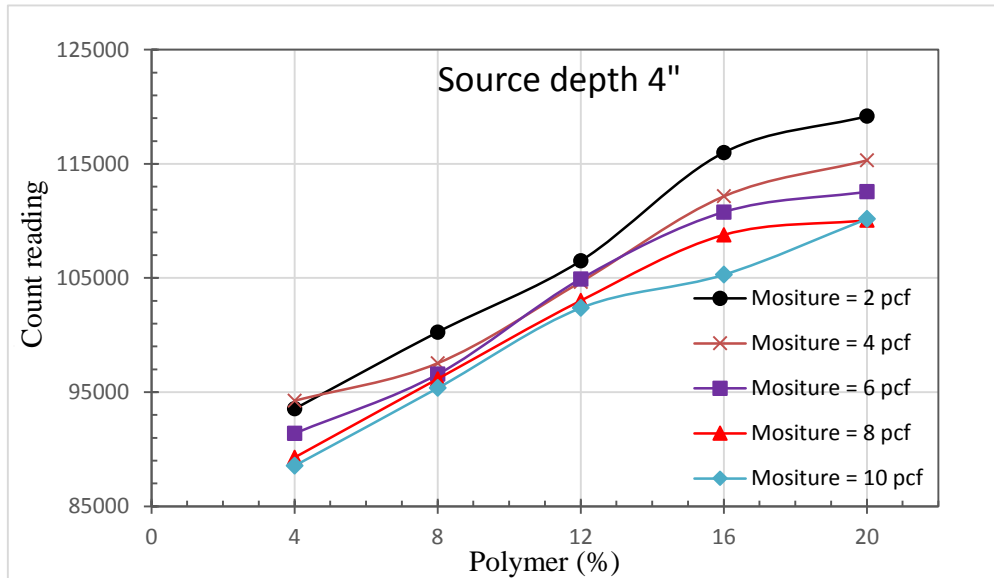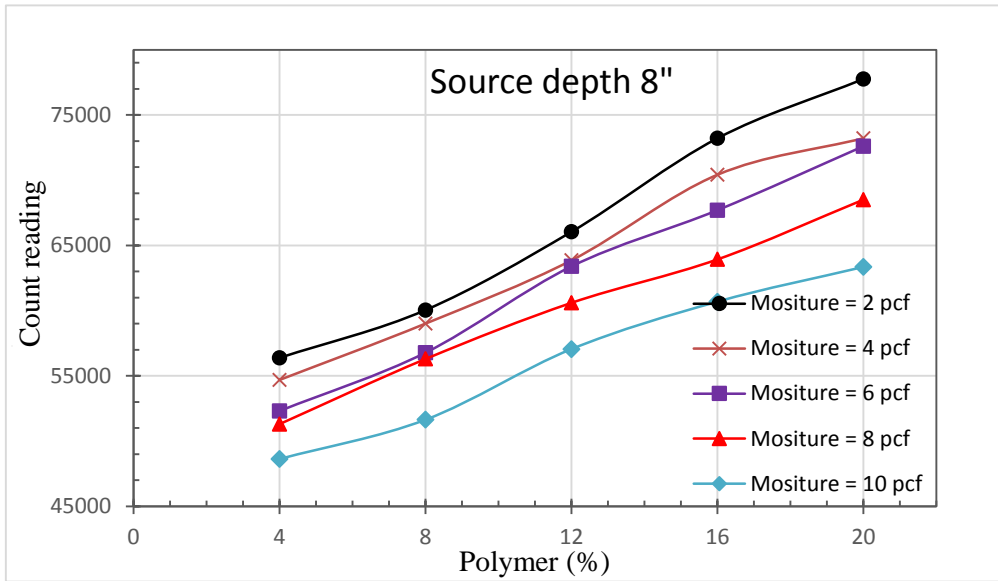
Figure 13. Photon counting reading with different polymer volume fraction at BC=4″ at different source depths.
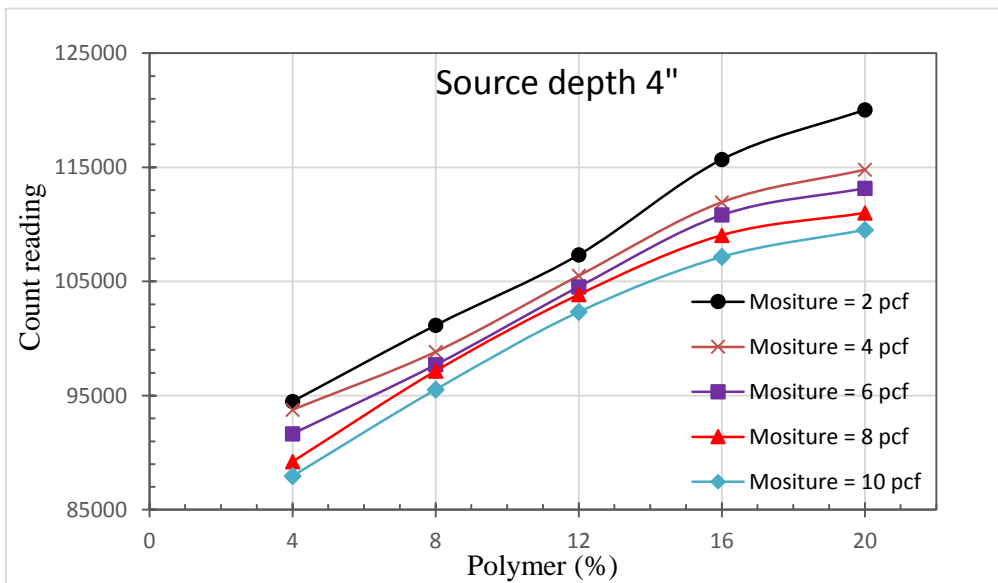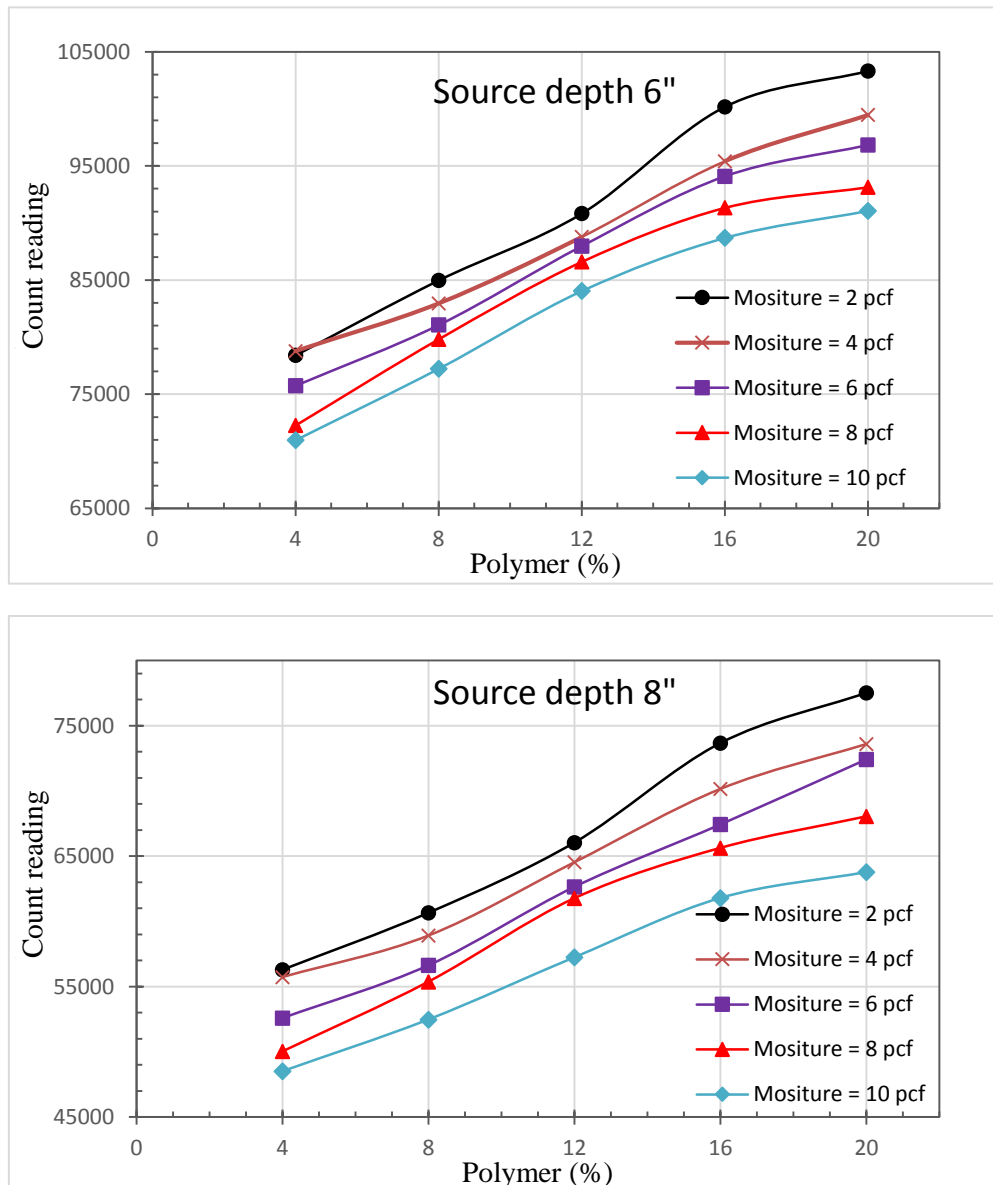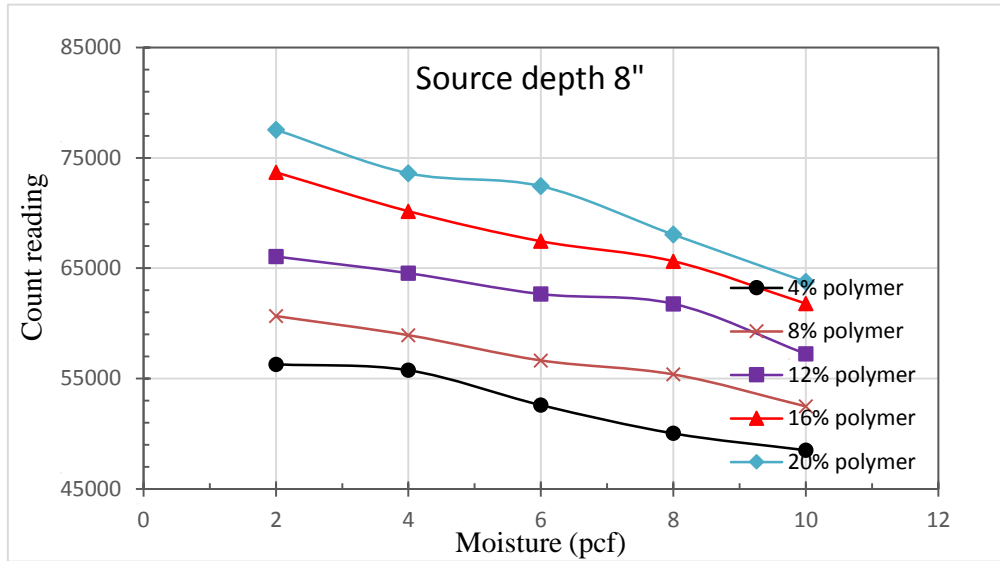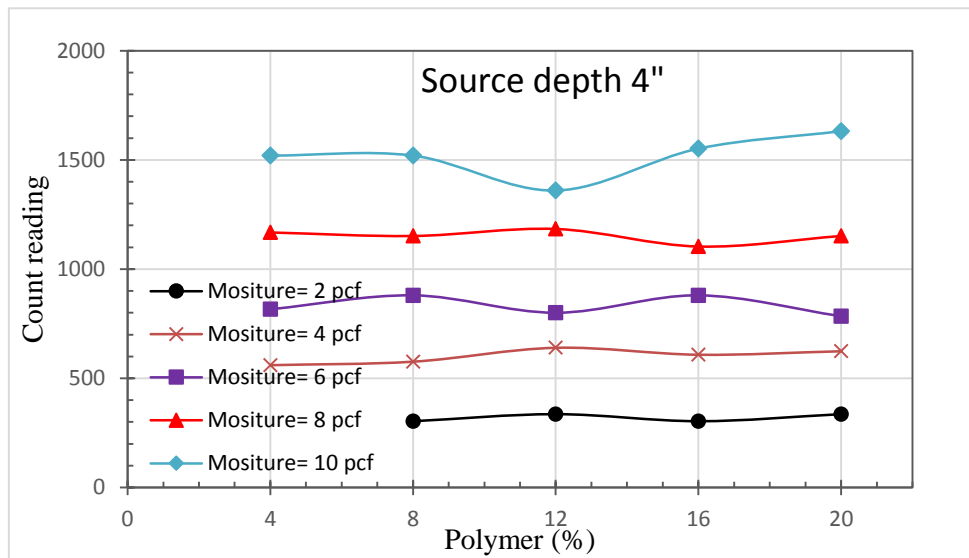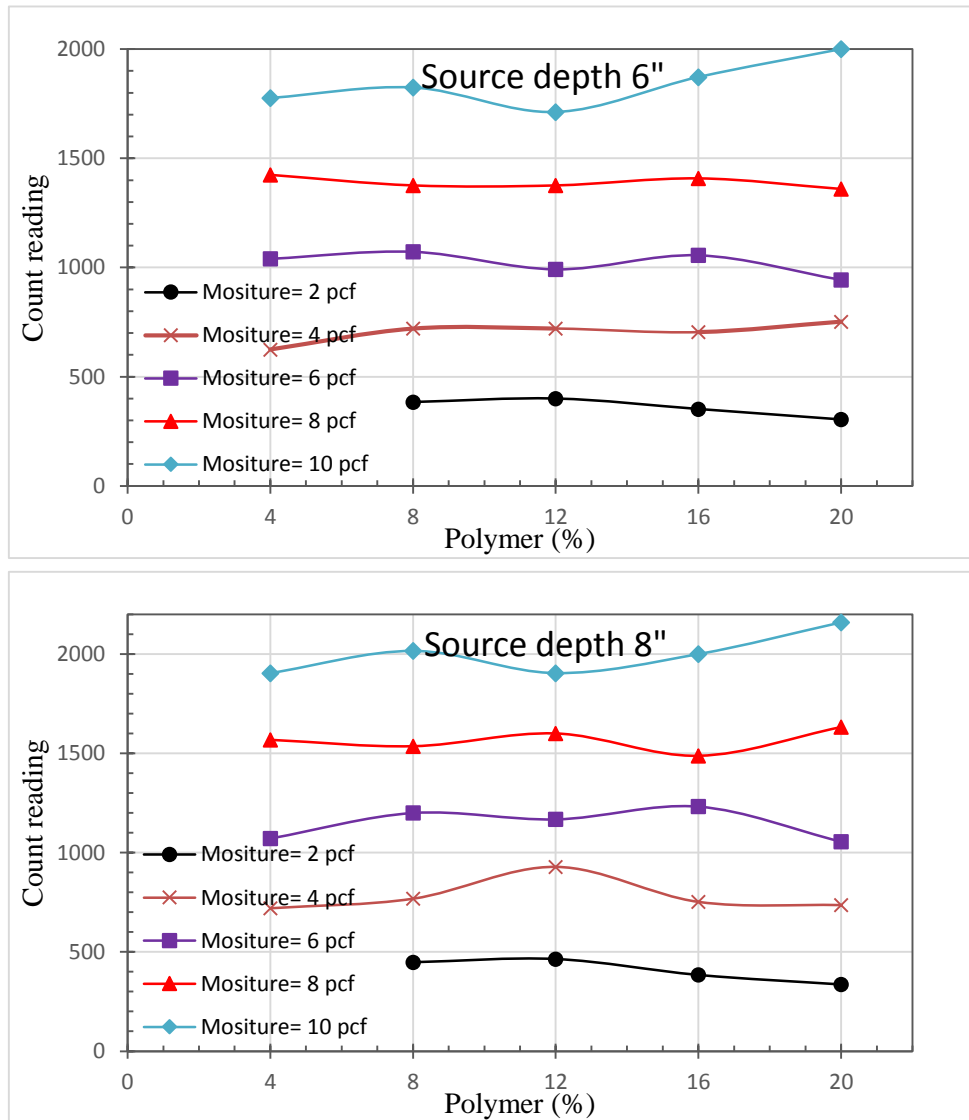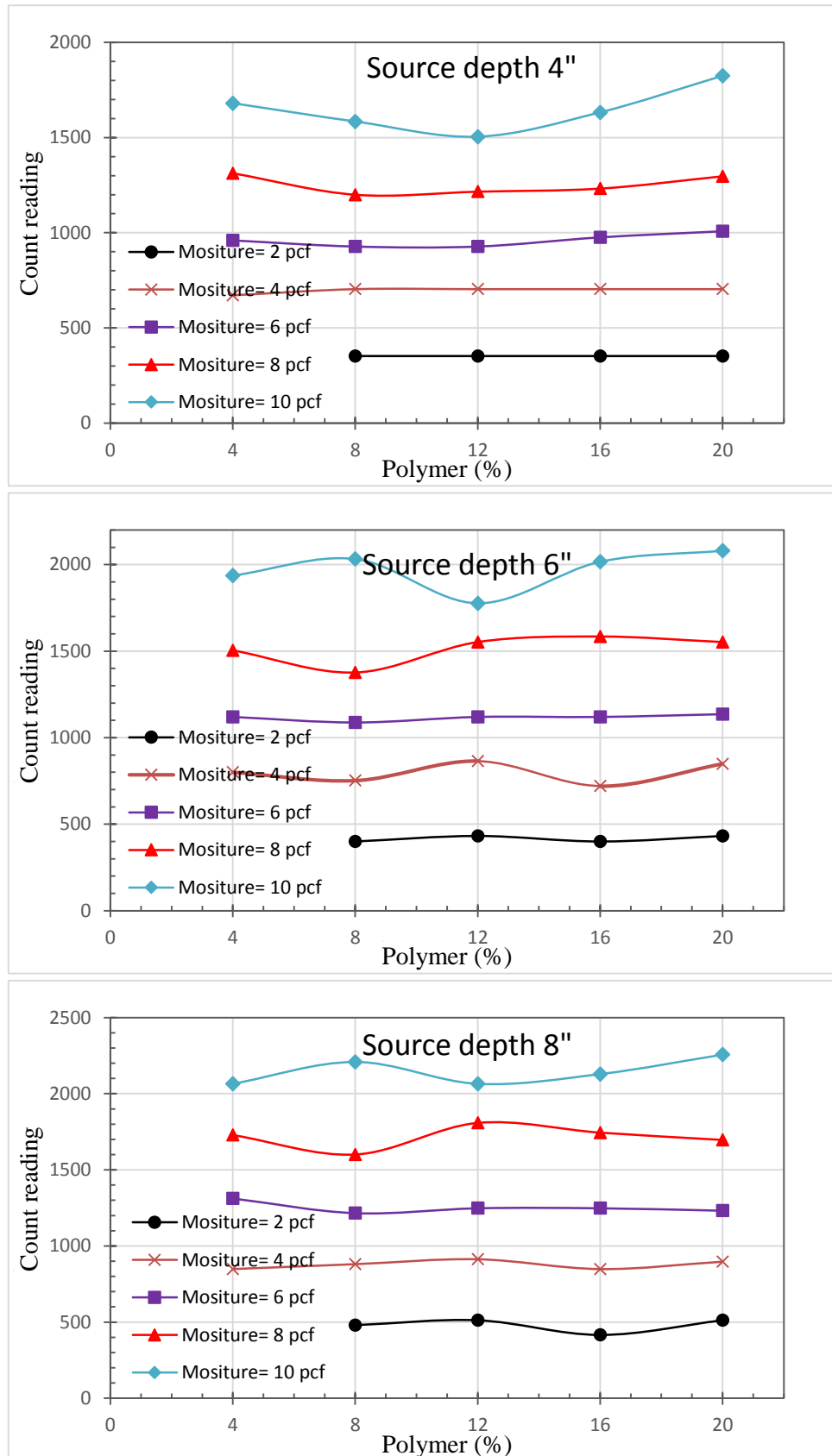
Figure 14. Photon counting reading with different polymer volume fraction at BC=6″ at different source depths.

The variances of the counting readings with respect to different moisture contents at different boundaries are shown in Figure 15 to **Error! Reference source not found.**.   For each sample with the same amount of polymer and sand, the density of the sample increases as the added water content increases, therefore, as expected, the photon count number continually decreases as the moisture content gradually increases.   Along the vertical direction, Figure 15 and Figure 16 show that at each moisture content, the photon count number increase as the polymer volume fraction increases since their density gradually decreases.

For the neutron reading, it shows from **Error! Reference source not found.** and **Error! Reference source not found.** that the neutron count number increases in an approximately linear pattern as the moisture content increases, and that all the cures for different polymer volume fractions almost merge together. It demonstrates that the neutron count number are

only proportional to the moisture content of the sample while independent on the sample density. Again, Figure 15 to Figure 20 show that the boundary effects on both the photon and neutron readings are negligible.
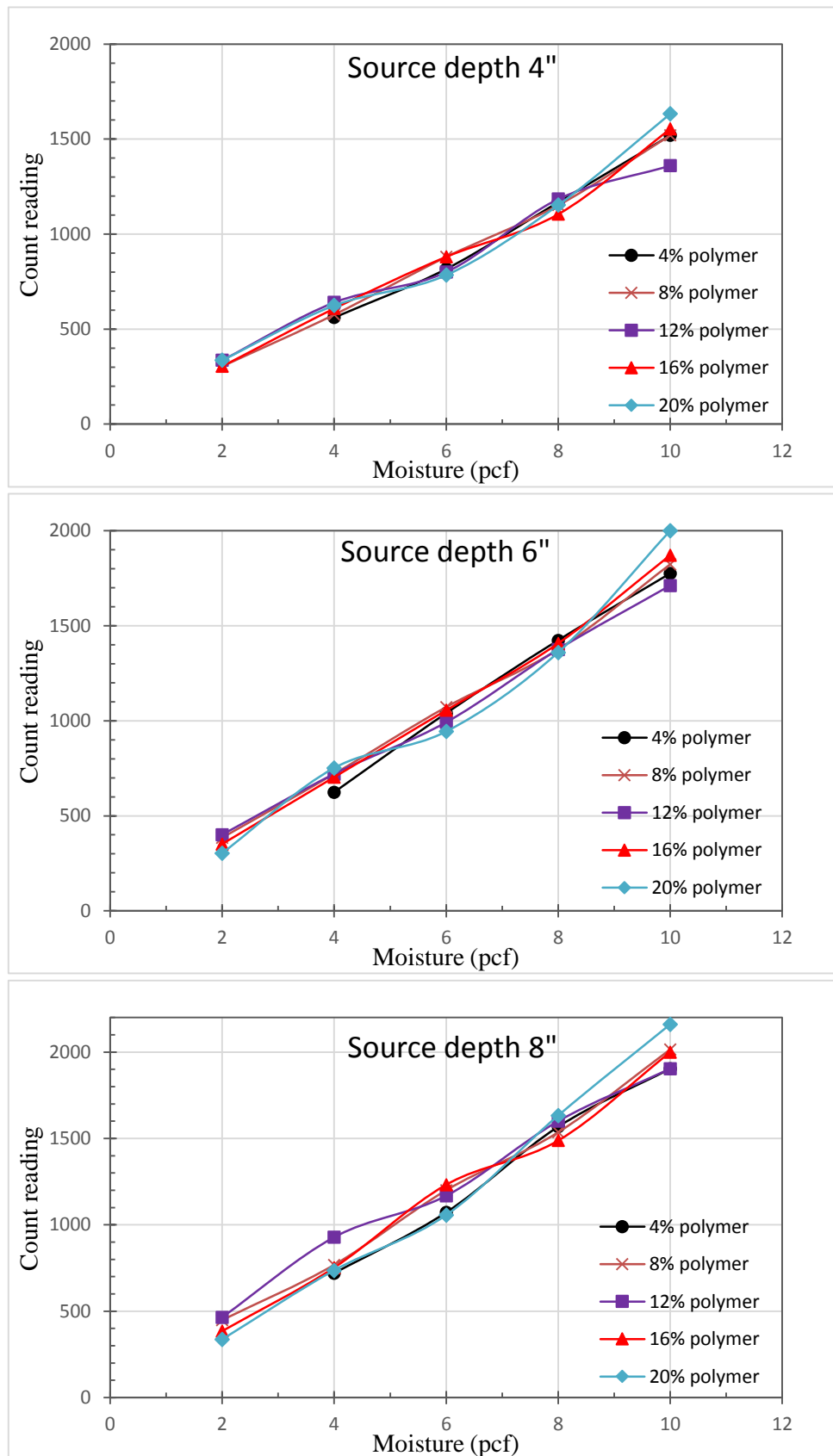
Photon reading V.S. Moisture
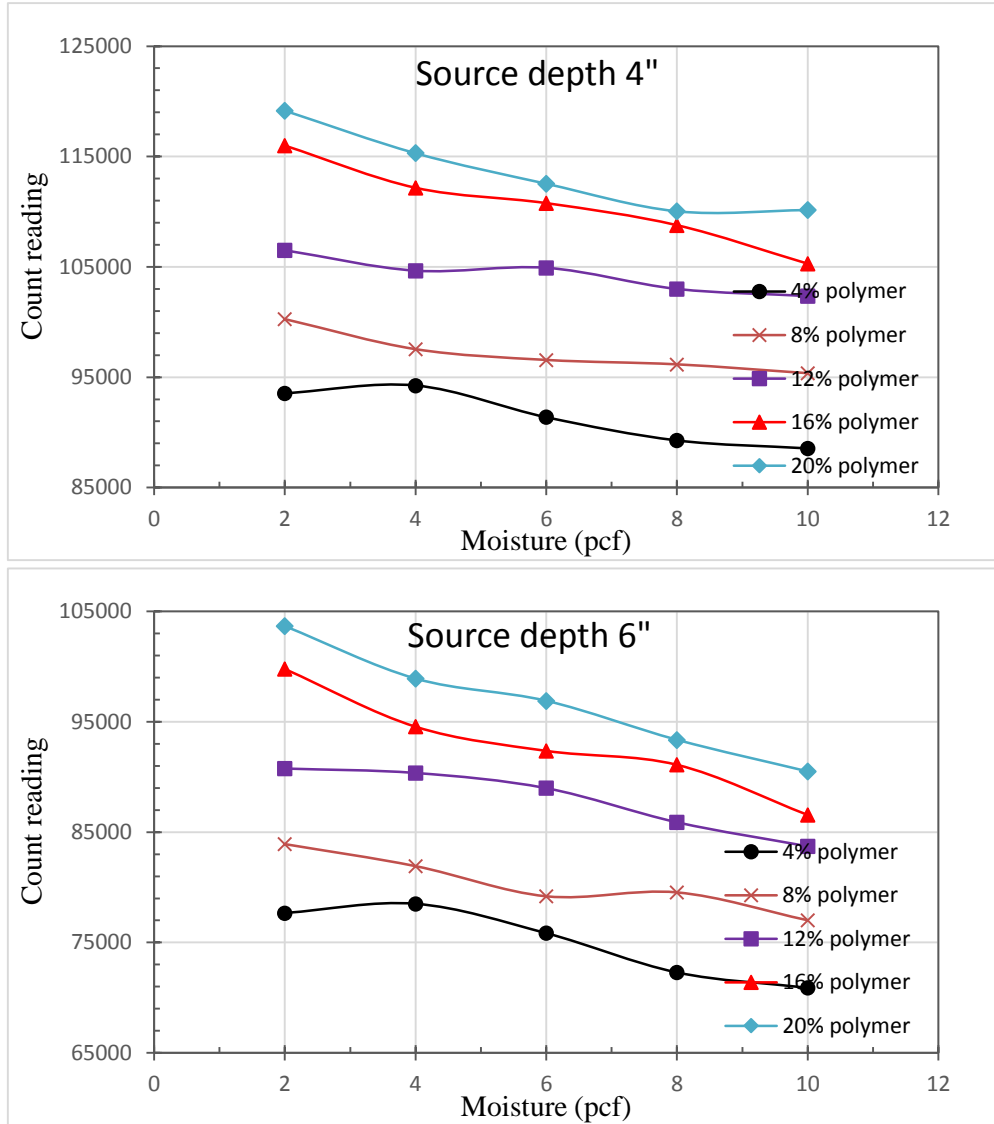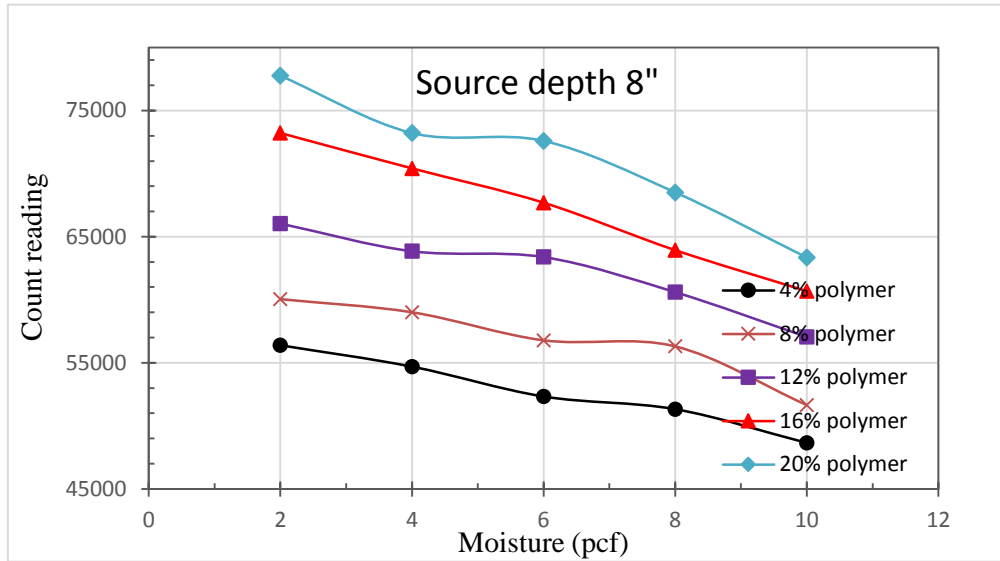
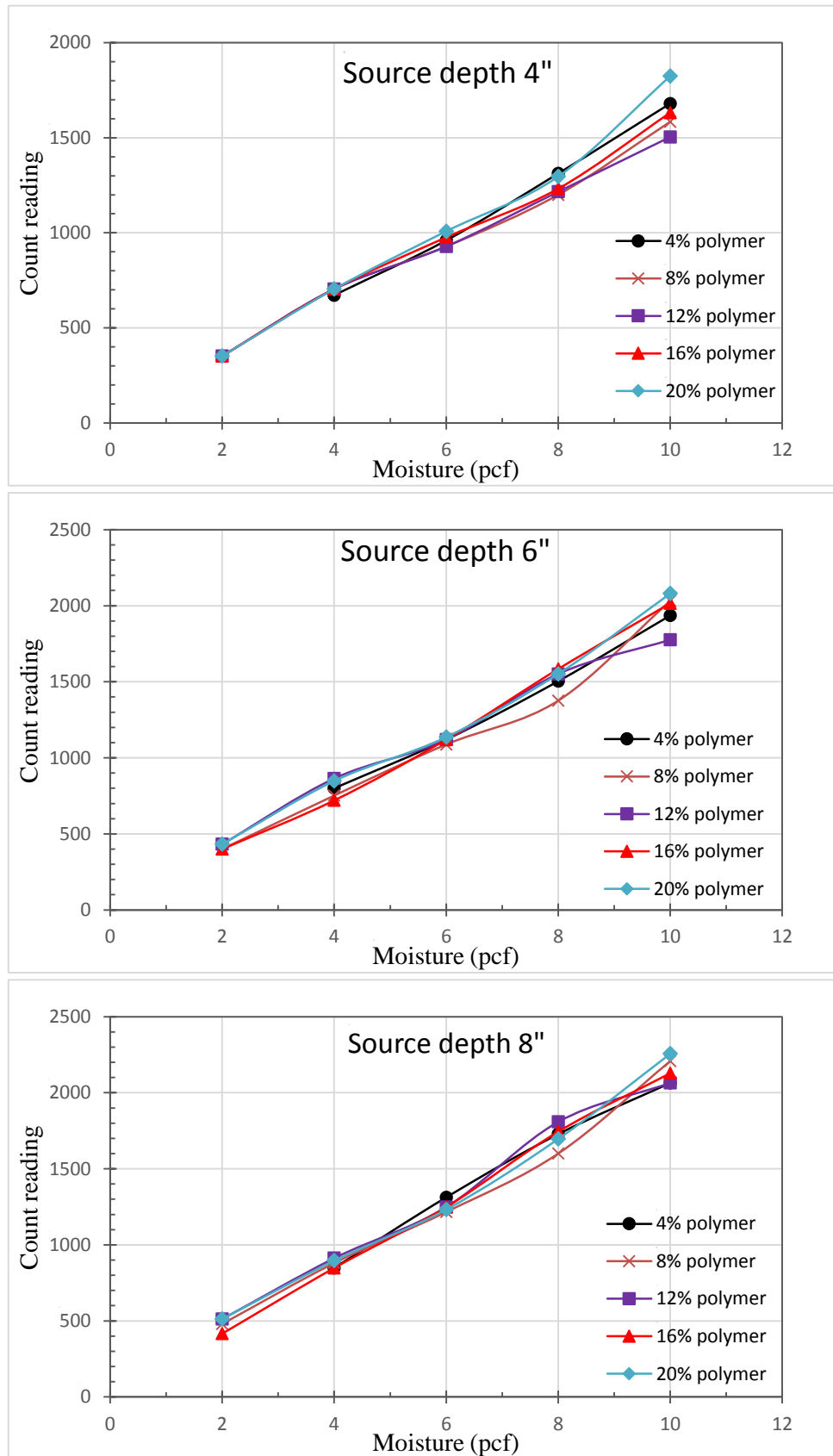Figure 15. Photon counting reading with different moisture contents at BC=4″ at different source depths.
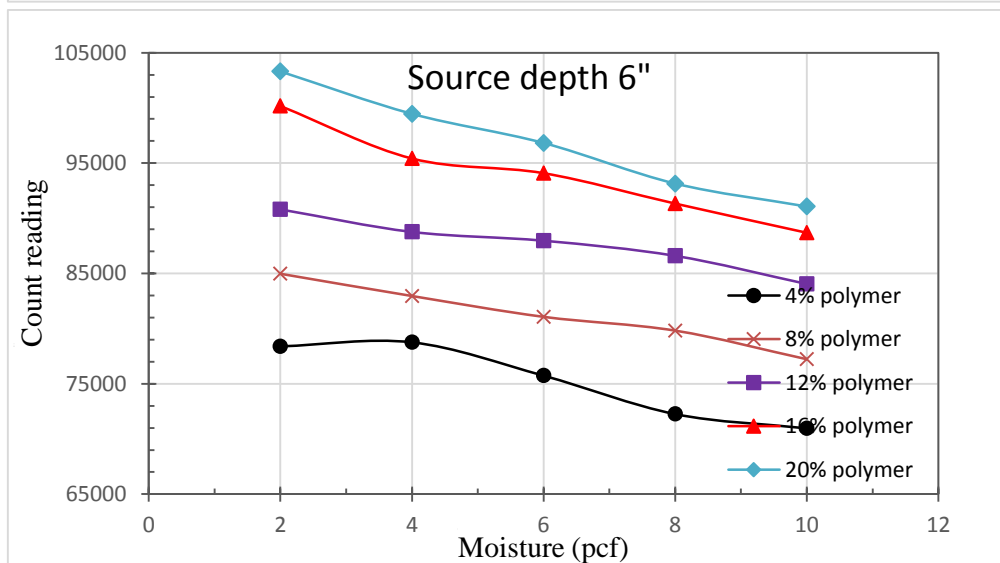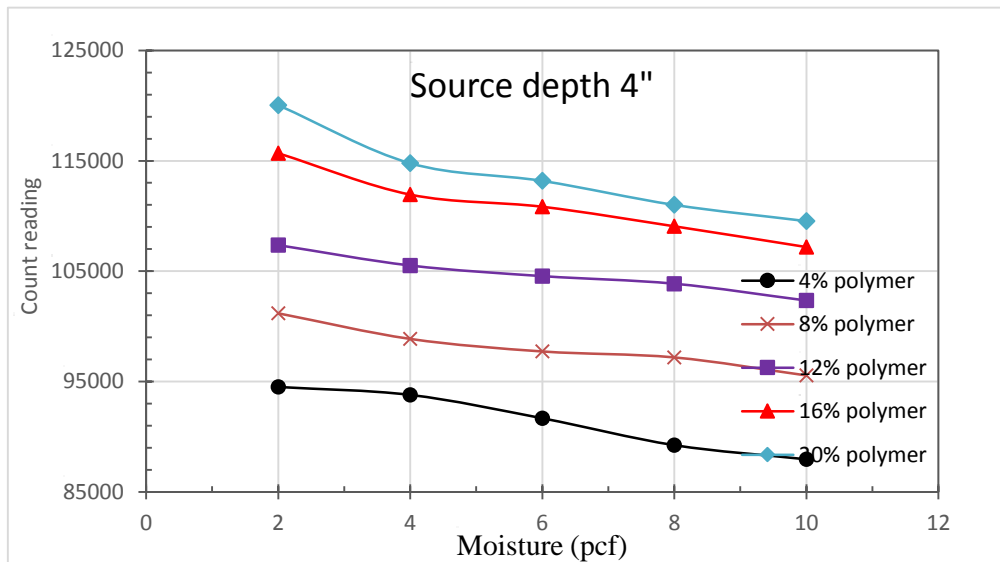
Figure 16. Photon counting reading with different polymer volume fraction at BC=6″ at different source depths.

Neutron reading V.S. Polymer

Figure 17. Neutron counting reading with different polymer volume fraction at BC=4″ at different source depths.

Figure 18. Neutron counting reading with different polymer volume fraction at BC=6″ at different source depths.

Neutron reading V.S. Moisture

Figure 19. Neutron counting reading with different moisture contents at BC=4″ at different source depths.

Figure 20. Neutron counting reading with different moisture contents at BC=6″ at different source depths.

5.4 Data analysis

5.4.1 Decouple of photon attenuation of hydrogen from other types of atoms.

When a well-collimated nuclear gauge with a narrow energy range is used, the gamma ray beam due to the absorption or scattering of the beam is attenuated in accordance with an exponential function, which is the same as the radioactive decay function and can be expressed as[39]:

$$CN = a' * exp(-b'\text{D}) \tag{15}$$

A linear function in the semi-logarithmic coordinate can represent the above relation as

$$ln(CN) = a - b * D \tag{16}$$

where $a = \ln(a')$ and $b = b'$ corresponding to Eq. (15).

Based on the photon reading number for the samples with the same moisture content but with different volume fractions of polmer particles, the variances of the density with respcet to the logarithmic counting number for different moisture contents at BC = 4″ and 6″ are shown in Figure 22 and Figure 22, respectively. Overall, except the end part when the *ln (CN)* is relative large, the most part of these curves are in a linear trend. Linear regression analysis are conducted by the linear curve fitting ($ln(CN) = a - b * D$). The constants of *a* and *b* in Eq. (16) are obtained by the linear regression analysis and the analysis results are provided in
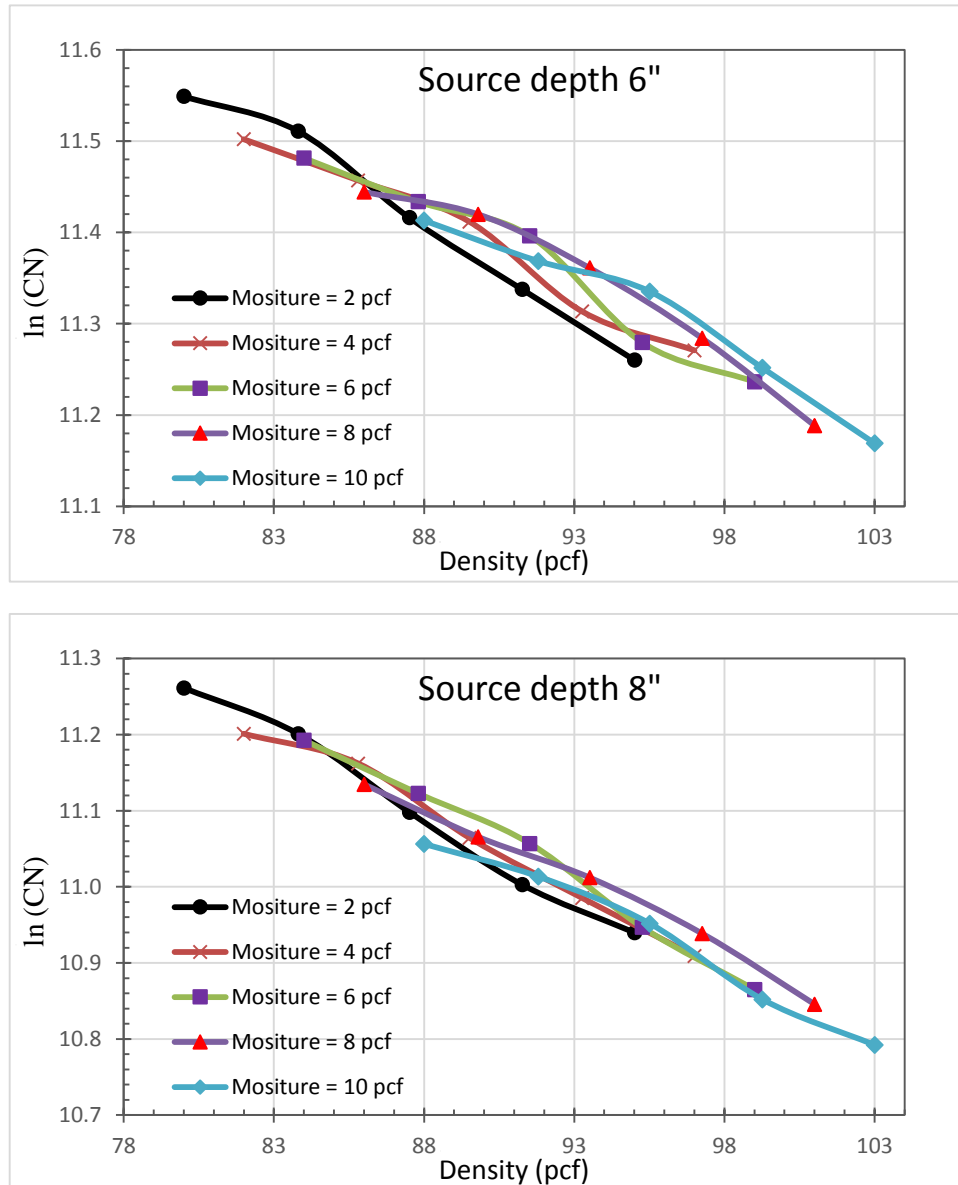
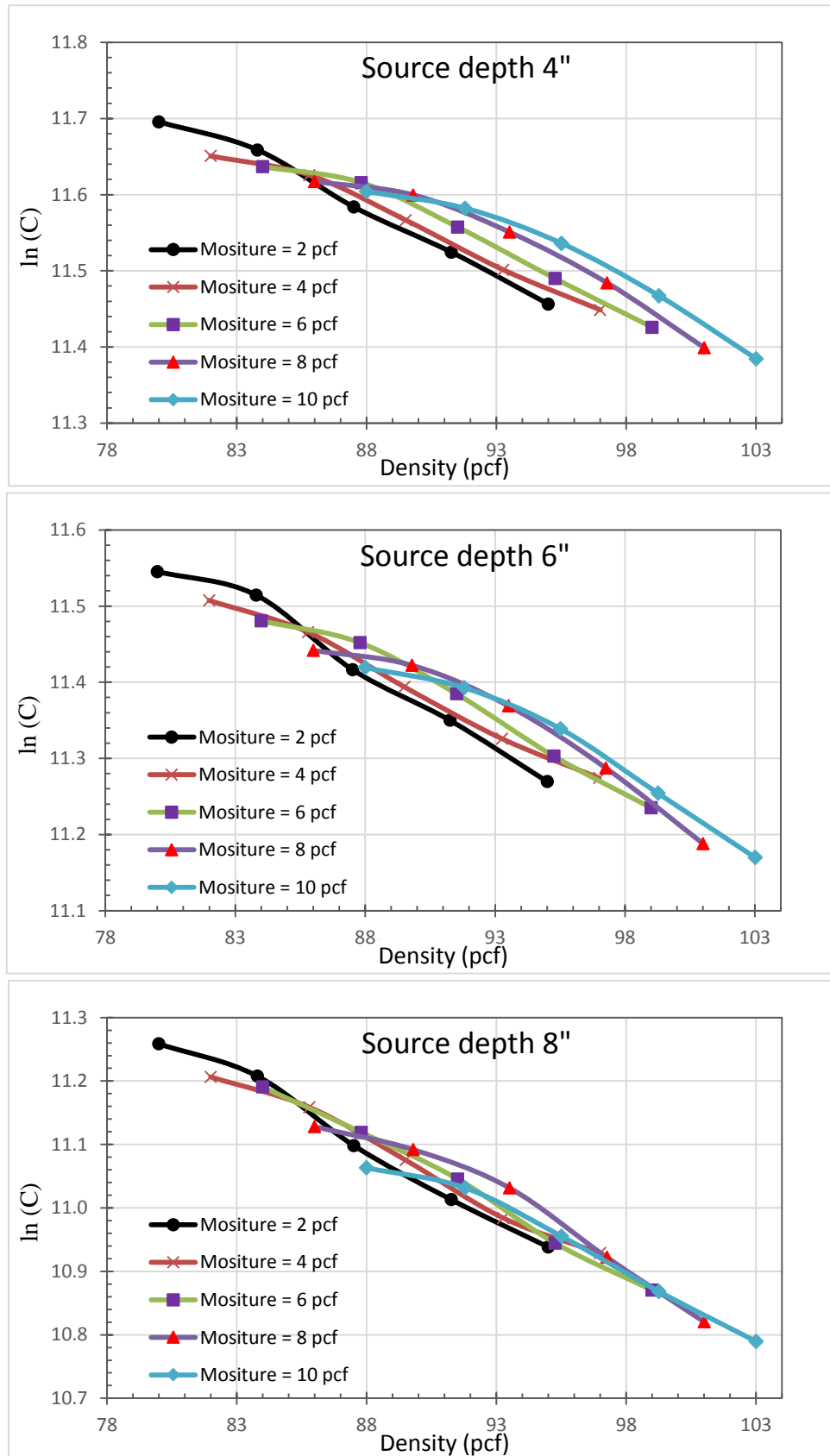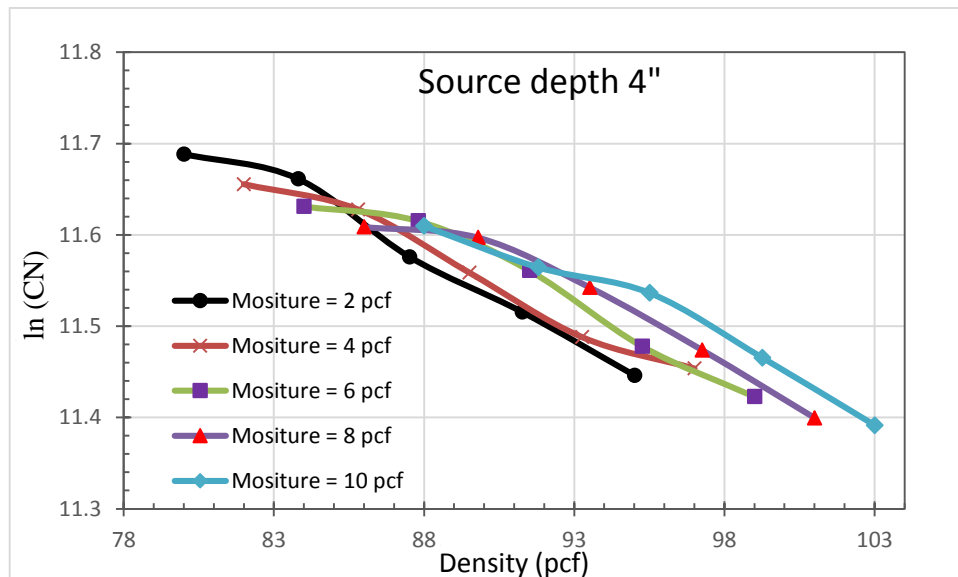Figure 21 Variances of the density with respcet to ln (CN) for different source depthes at BC = 4″.

Figure 22 Variances of the density with respcet to ln (C) for different source depthes at BC = 6″.

In order to decouple the photon reading numbers from the two parts (dry sample and moisture) shown in Eq. (15), the counting number for the dry sample need to be predicted first. It is assumed that the hydrogen only comes from the moisture in the sand and that there is no moisture in the dry sample. As previously stated in the mixing design part, it is not practicable to mix the sand with different amount of polymer particle at dry condition, thus the density-*ln(CN)* curve at moisture = 0 pcf is not practicable available in this study.   However, it shows from Figure 22 that the curve shapes for different moisture contents are quite similar and the slopes (*b*) obtained from the linear regression are close. Considering that the natural errors resulted from the laboratory testings might also contribute those discrepancies of *b* among different samples, we assume that all the curves for samples with different moisture share the same slope (i.e., they have the same *b* value). From a statistical point of view, we take an average value for all the samples, i.e., $b_0 = \sum_{i=1}^{5} b^i /5$.   By fixing this constant slope ($b = b_0$), one more regression analysis is further conducted by the linear curve fitting ($\ln(CN) = a_0 - \sum_{i=1}^{5} b^i /5 * D$ to evaluate the viability of this curve fitting quality. The updated regression results are presented in **Error! Reference source not found.**. Based on the updated regression results, an individual straight line for each sample with different moisture contents (2, 4 … 10 pcf) can be determined, and thus the one for the "imaginary" sample without moisture can be obtained by a linear interpolation as shown in Figure 23 which provides that $a_0 = 12.871, 12.926,$ and 12.908 for the counting readings with different radiation source depths, respectively. Therefore, the density of the dry sample without moisture can be deduced as $\ln(CN) = a_0 - b_0 * D$.

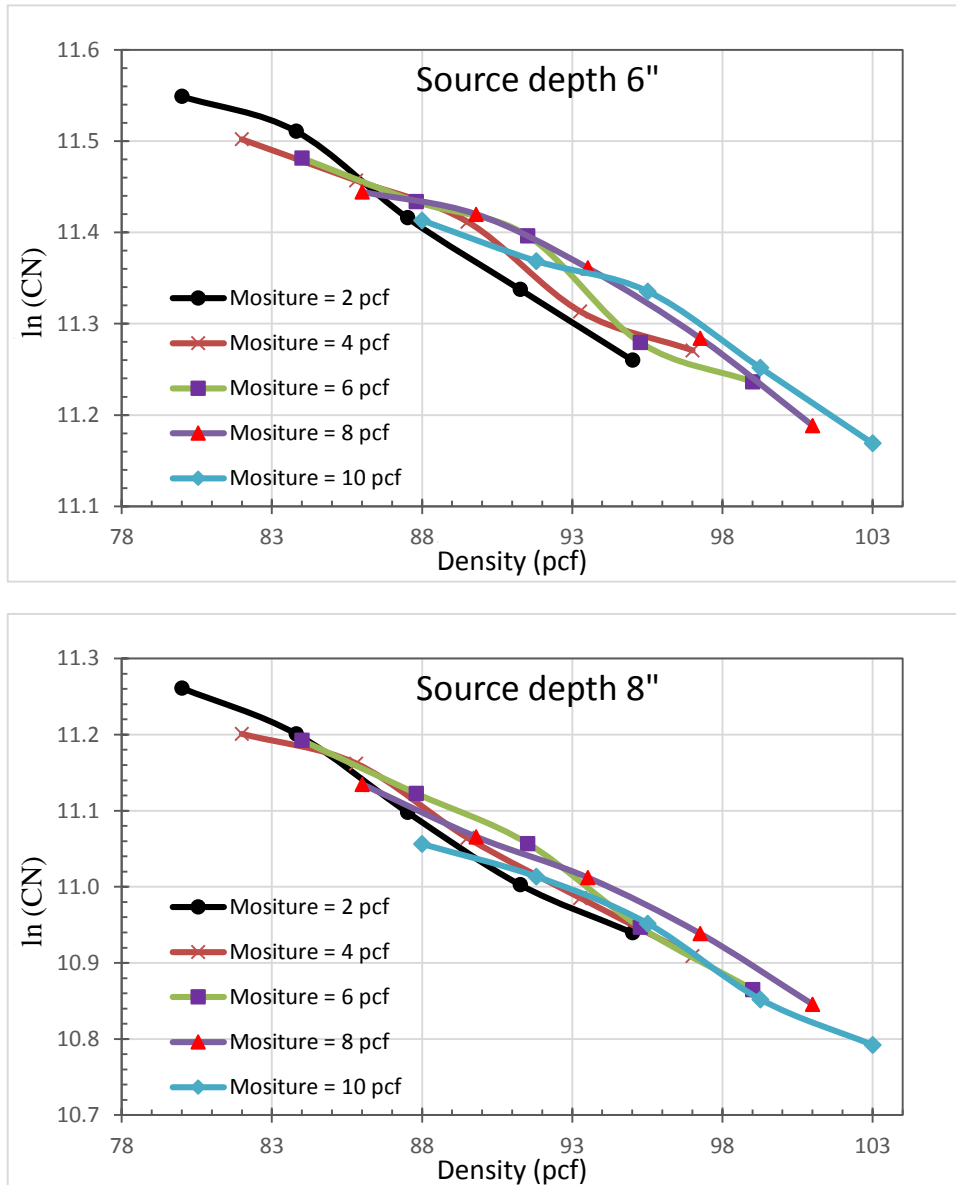Table 9. The higher R_0^2 indicates that the density-*ln(CN)* fits in a good linearity.

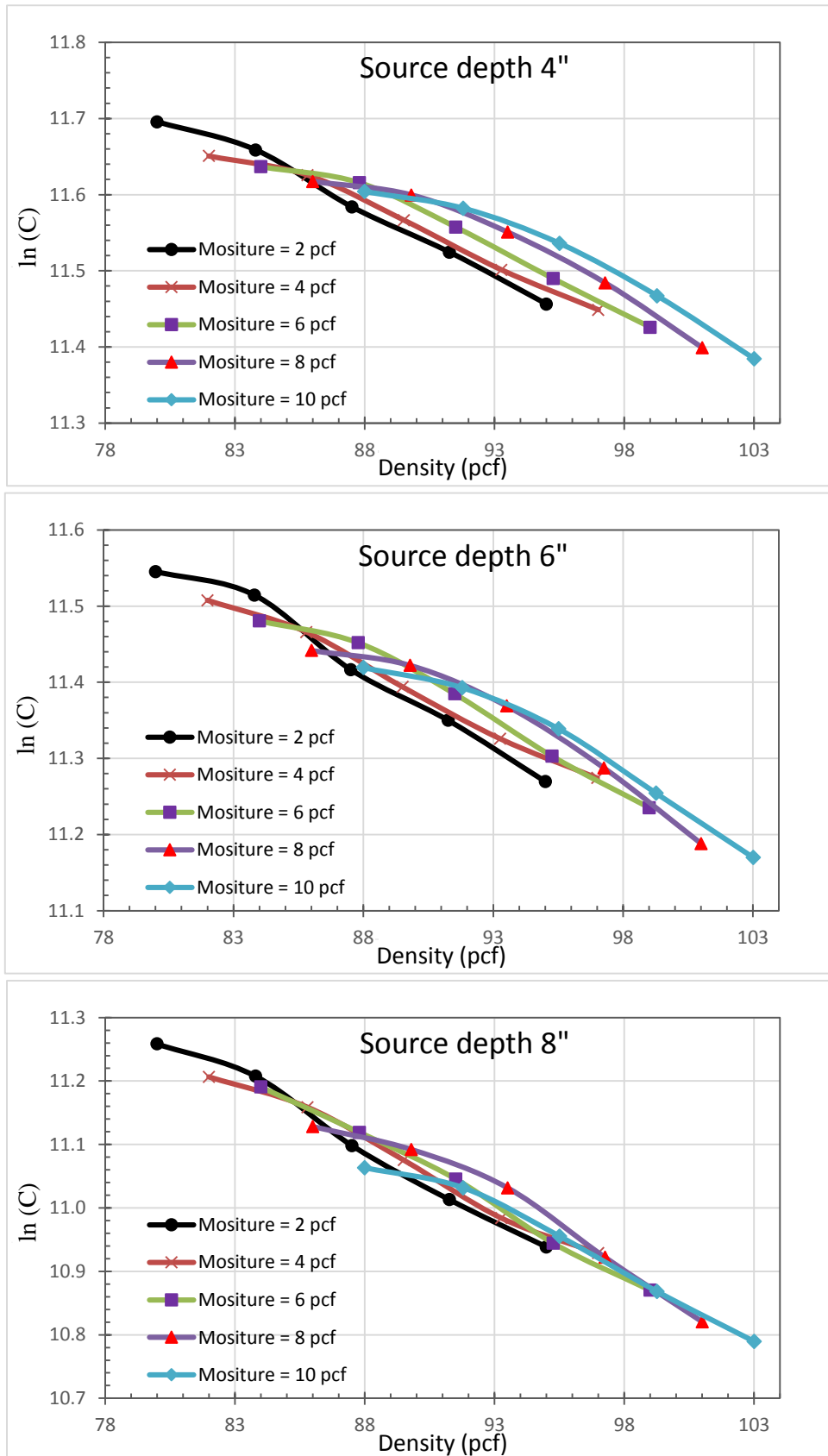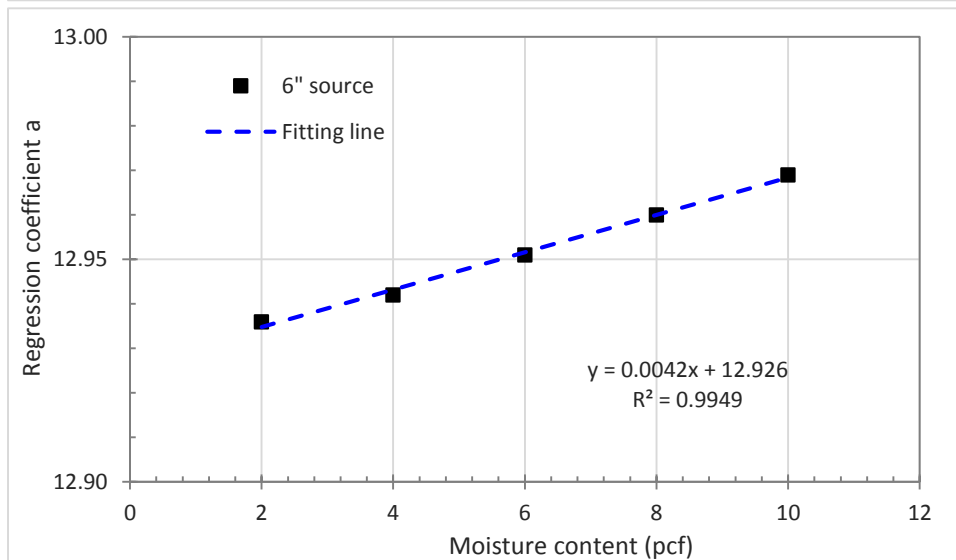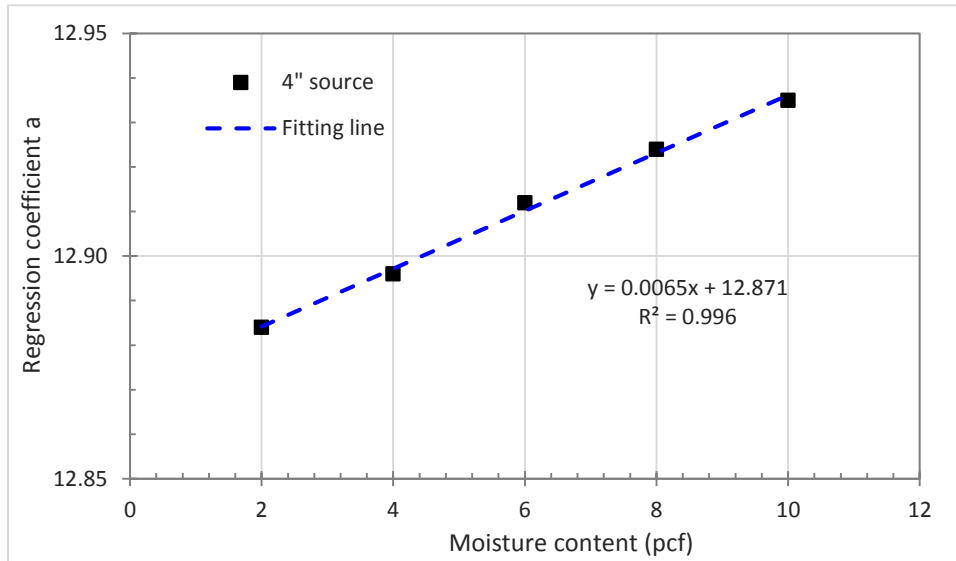Figure 21 Variances of the density with respcet to ln (CN) for different source depthes at BC = 4″.

Figure 22 Variances of the density with respcet to ln (C) for different source depthes at BC = 6″.

In order to decouple the photon reading numbers from the two parts (dry sample and moisture) shown in Eq. (15), the counting number for the dry sample need to be predicted first. It is assumed that the hydrogen only comes from the moisture in the sand and that there is no moisture in the dry sample. As previously stated in the mixing design part, it is not practicable to mix the sand with different amount of polymer particle at dry condition, thus the density-*ln(CN)* curve at moisture = 0 pcf is not practicable available in this study.   However, it shows from Figure 22 that the curve shapes for different moisture contents are quite similar and the slopes (*b*) obtained from the linear regression are close. Considering that the natural errors resulted from the laboratory testings might also contribute those discrepancies of *b* among different samples, we assume that all the curves for samples with different moisture share the same slope (i.e., they have the same *b* value). From a statistical point of view, we take an average value for all the samples, i.e., $b_0 = \sum_{i=1}^{5} b^i /5$.   By fixing this constant slope ($b = b_0$), one more regression analysis is further conducted by the linear curve fitting ($\ln(CN) = a_0 - \sum_{i=1}^{5} b^i /5 * D$ to evaluate the viability of this curve fitting quality. The updated regression results are presented in **Error! Reference source not found.**. Based on the updated regression results, an individual straight line for each sample with different moisture contents (2, 4 … 10 pcf) can be determined, and thus the one for the "imaginary" sample without moisture can be obtained by a linear interpolation as shown in Figure 23 which provides that $a_0 = 12.871, 12.926,$ and 12.908 for the counting readings with different radiation source depths, respectively. Therefore, the density of the dry sample without moisture can be deduced as $\ln(CN) = a_0 - b_0 * D$.

Table 9. Regression analysis results for $\ln(CN) = a - b * D$.

Source Depth	Moisture (pcf)	Initial regression			Second regression		
		a	b	R^2	a_0	b_0	R_0^2
4"	2	13.0146	0.01635	99.07%	12.884	0.01491	98.3%
	4	12.82087	0.01410	98.21%	12.896	0.01491	97.9%
	6	12.88219	0.01461	97.26%	12.912	0.01491	97.2%
	8	12.90734	0.01473	94.67%	12.924	0.01491	94.7%
	10	12.92575	0.01477	95.25%	12.935	0.01491	95.2%
6"	2	13.09090	0.01910	98.17%	12.936	0.01730	97.3%
	4	12.84171	0.01618	99.29%	12.942	0.01730	98.8%
	6	12.93314	0.01707	97.78%	12.951	0.01730	97.8%
	8	12.94423	0.01714	94.08%	12.960	0.01730	94.1%
	10	12.93857	0.01700	96.04%	12.969	0.01730	96.0%

8"	2	13.0526088	0.02228	99.02%	12.910	0.02068	98.5%
	4	12.8143941	0.01948	98.93%	12.915	0.02068	98.6%
	6	13.0233588	0.02174	99.61%	12.925	0.02068	99.4%
	8	12.9569056	0.02094	96.02%	12.930	0.02068	96.0 %
	10	12.7516533	0.01895	97.84%	12.924	0.02068	97.0%

$y = 0.0065x + 12.871$
$R^2 = 0.996$

$y = 0.0042x + 12.926$
$R^2 = 0.9949$
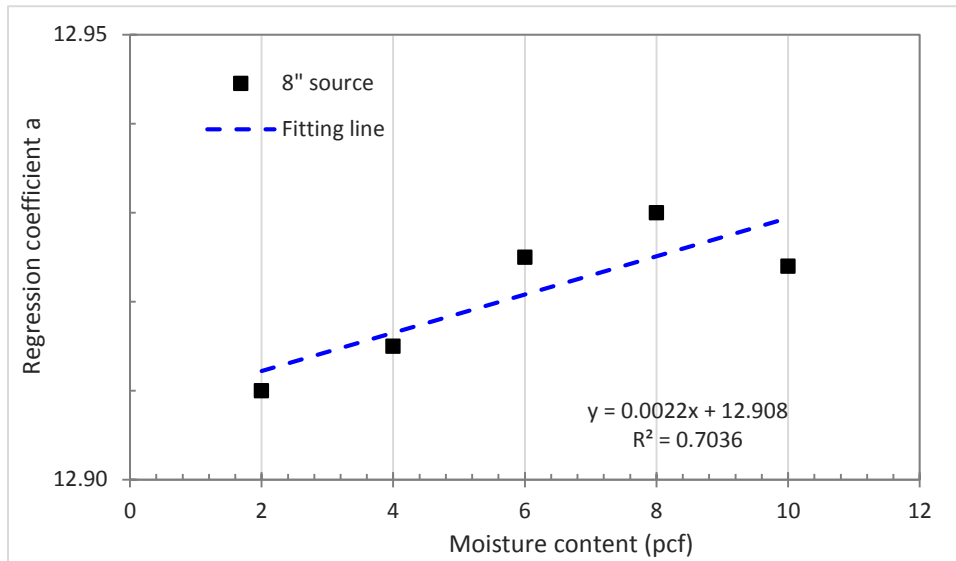
Figure 23. Interpolation to determine the dry sample fitting curve.

Figure 24 shows the variance of the value $\frac{\ln(CN)-(a_0-b_0*D)}{H}$ with respect to the density of the tested material with different moisture, where H is proportional to the moisture content per cubic feet as no other hydrogen resources are considered. Ideally this normalized term is supposed to be merged into a single value (a straight line in horizontal direction). However, because of the inevitable testing errors among other unknown reasons, certain fluctuations are observed in Figure 24, especially for the one with moisture content of 2 pcf which is obviously out of the trend. Nevertheless, the rest of samples (with moisture of 4, 6, 8 and 10 pcfs) are shown in a good trend and consistency. Therefore, the ideally converged one is assumed to the average of all the value shown in Figure 24 by excluding the first sample (with 2pcf moisture content), i.e., k = 6.368e-3, 4.263e-3 and 2.609 for the three source depths 4", 6" and 8", respectively.
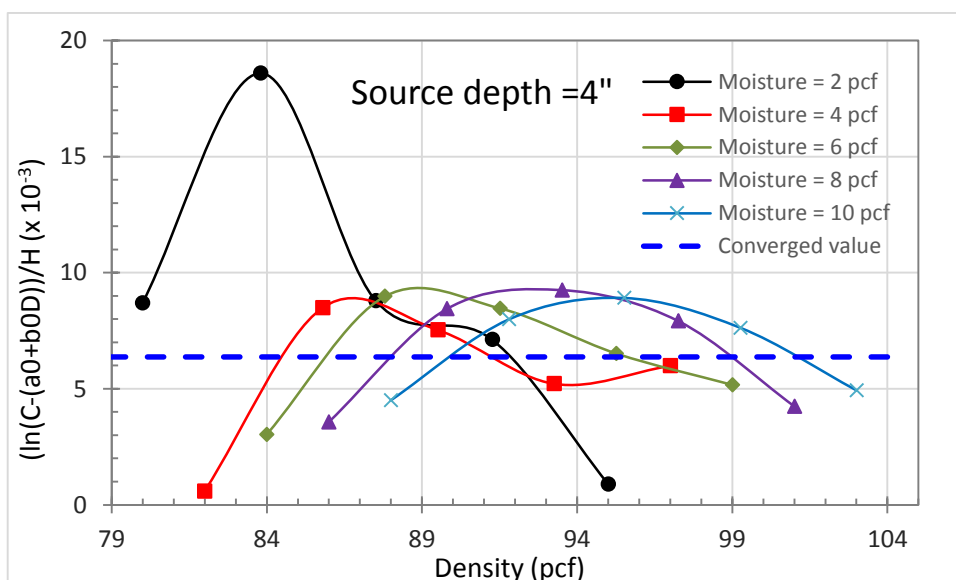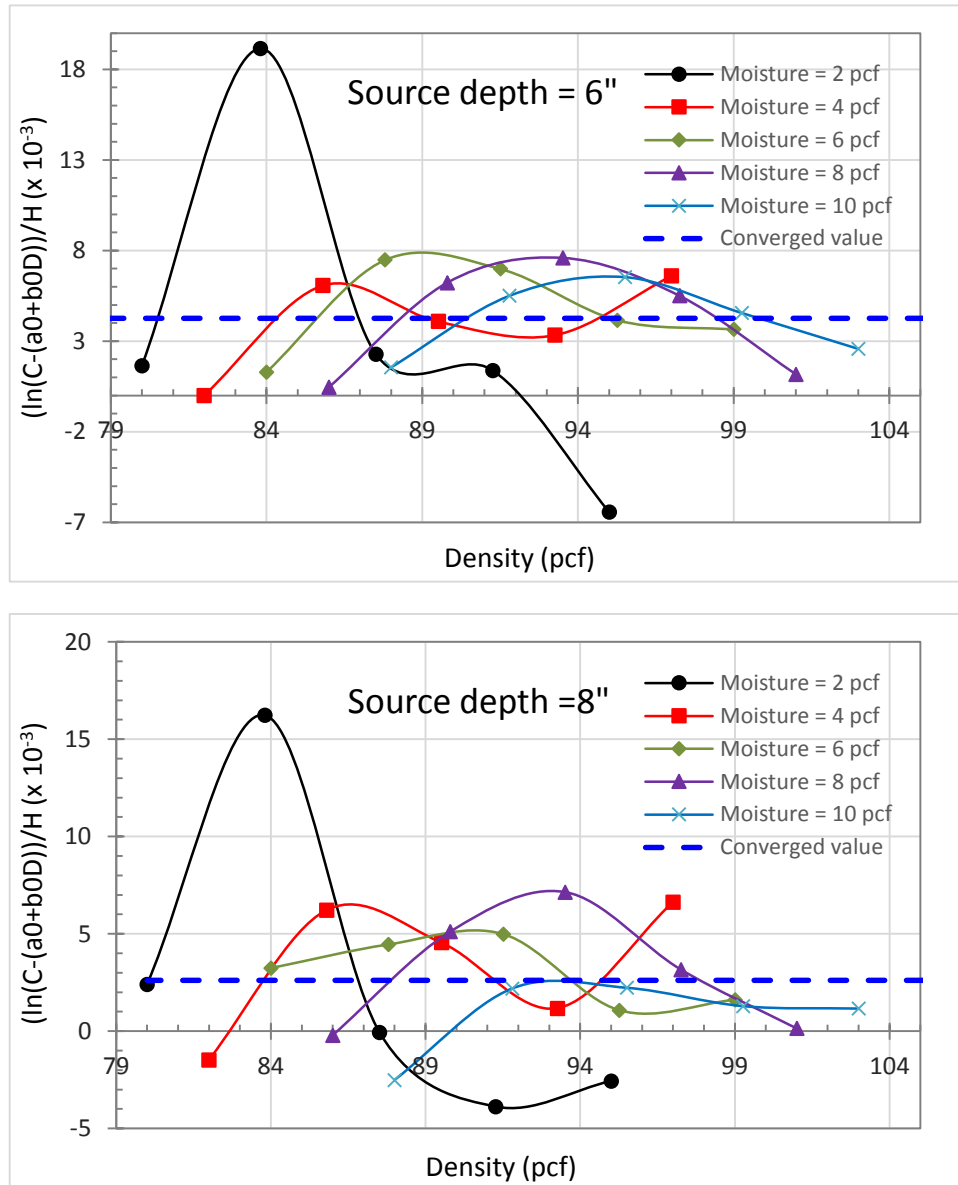
Figure 24. Variance of the relative density ratio $\frac{D-(a_0-b_0*ln(CN))}{H}$ with respect to the density of the tested materials with different moisture contents.

Based on this converged value k, the relationship among the count number, density and the moisture content of a tested sample can be eventually established by the following equation:

$$\ln(CN) = b - k_1 D + k_2 H \qquad (17)$$

which can be used as a calibration function with the parameters b, k_1 and k_2 to be determined. Once they are calibrated with standard blocks, the density of a test sample can be determined as:

$$D = b/k_1 + k_2/k_1 H - \ln(CN)/k_1 \qquad (18)$$

5.4.2 Neutron attenuation

As shown in Figure 19 and Figure 20, the neutron count number increases proportionally as the moisture content increases while independent of the polymer volume fractions (densities). Therefore, the moisture content of a test material can be uniquely determined by the reading neutron count numbers once the moisture content (MC) - neutron count number (CN_{Ne}) coefficient is calibrated. In order to obtain this coefficient, linear regression analyses were conducted on the correlation between the neutron count numbers and the moisture content shown in Figure 19 and Figure 20. The regression results are provided in Table 10, it indicates that the MC- CN_{Ne} coefficient increases as the source depth increases. However, in each source depth, these coefficients are quite consistent as indicated by the small value of coefficient of variations (COV). Therefore, an average value is applied from the five individual samples for each source depth, which is summarized in Table 10. It also shows that the MC- CN_{Ne} coefficient of BC = 6"is slightly larger than that of BC = 4", indicating that the source boundary condition might have certain effects on the neutron count numbers.

Table 10 Regression analysis of the Moisture-neutron count number coefficients

Foam volume fraction (%)	Moisture-neutron count number coefficient					
	BC=4" with different source depths			BC=6" with different source depths		
	4"	6"	8"	4"	6"	8"
4	150.7	179.9	192.9	166.4	190.8	209.4
8	149.3	177.8	196.8	152.7	191.8	210.5
12	135.8	168.0	188.1	147.7	178.5	207.8
16	149.0	184.0	197.0	158.2	200.5	214.6
20	153.8	190.9	214.4	175.1	200.7	216.7
Ave.	**147.7**	**180.1**	**197.8**	**160.0**	**192.4**	**211.8**
COV	**4.7%**	**4.7%**	**5.0%**	**6.8%**	**4.7%**	**1.8%**

5.4.3 Final decoupled model for density measurement

Based on the MC - CN_{Ne} coefficient obtained in Table 10 and the recorded neutron count numbers provided in Table 8, the hydrogen (in an equivalent form of moisture content) can be determined by $MC = CN_{Ne}/\lambda$. Therefore, once the photon and neutron count number readings are available, the density of a test material can be uniquely determined by these two readings through Eq. (19) as

$$D = k_1 - k_2 \ln(CN) + k_h CN_{Ne} \tag{19}$$

where $k_h = {k_0}/{\lambda}$ reflecting the hydrogen (or moisture) effect on the density measurement based on the neutron count numbers.

6. IMPROVED NUCLEAR TEST METHOD AND DEMONSTRATION

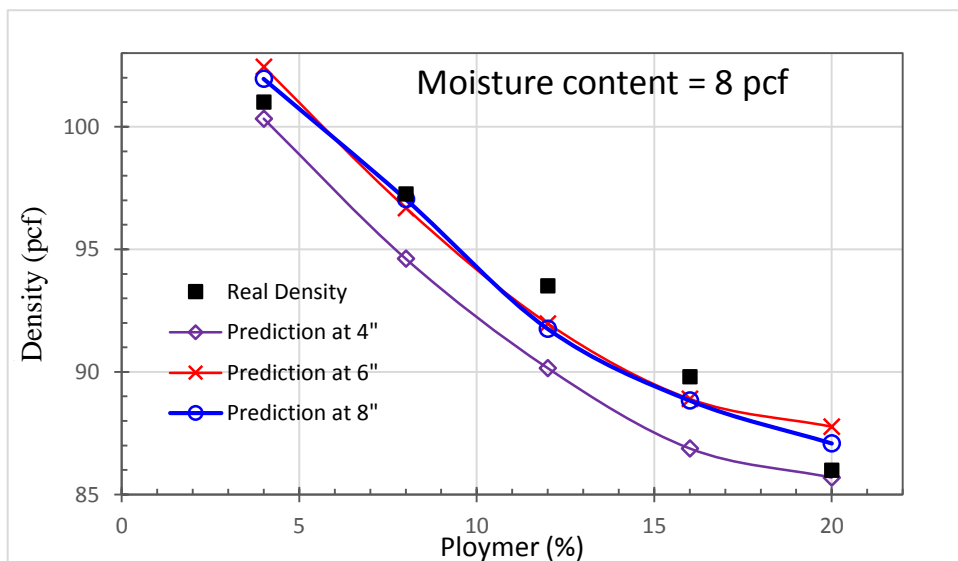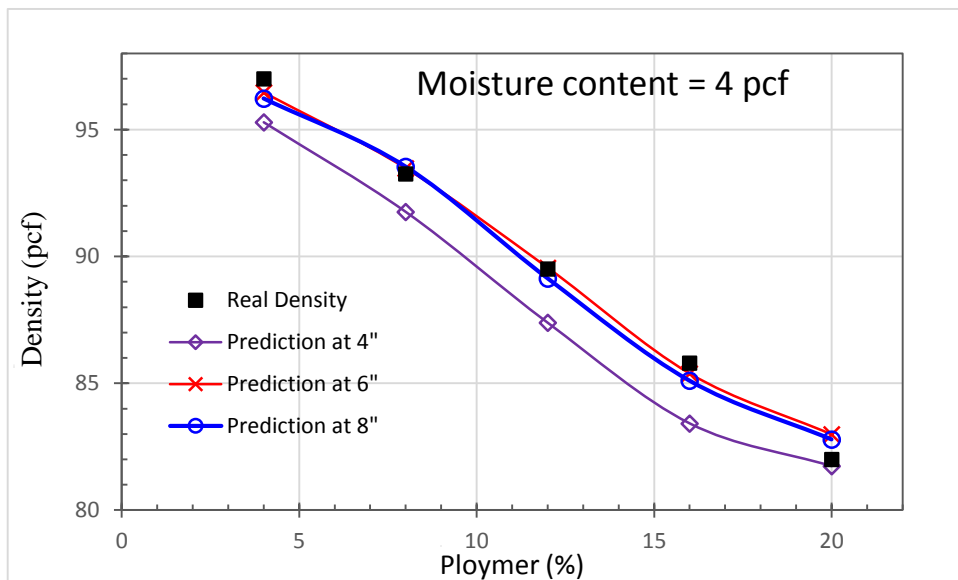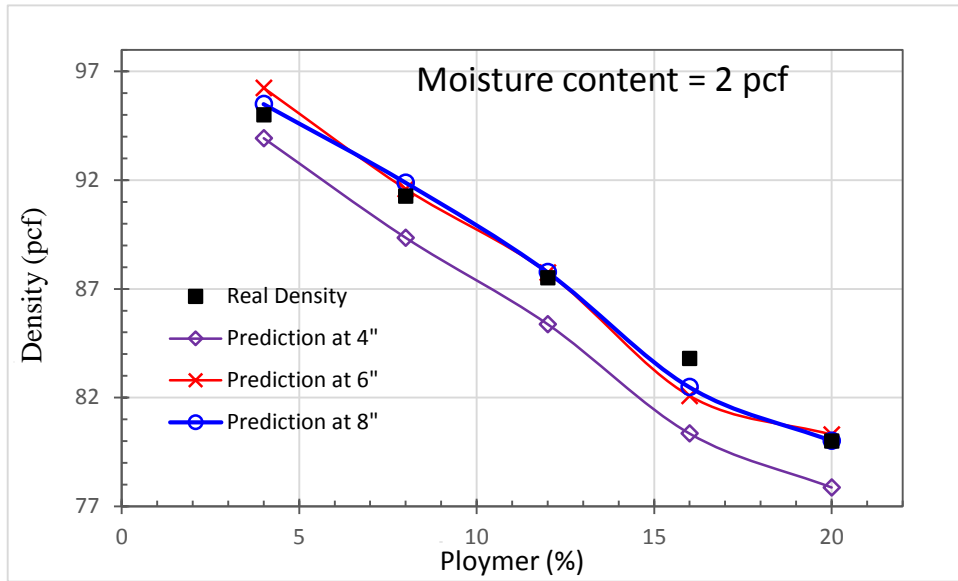### 6.1 Density prediction of the mixed sand composites

Based on the discovery of this function of CN related to D and H in Eq. (17), we can develop a new calibration method of the nuclear gages with a minimum of 3 calibration blocks including one aluminium (2.7g/cc), one magnesium (1.74g/cc) and one polymer blocks (say 0.95g/cc) with hydrogen content known (say 14.3 wt%). The first two can be used to determine k_1 and b, whereas the last one can be used to determine k_2. Redundant blocks can be used to reduce the accidental errors and improve the accuracy. At the same time, the last two blocks can be used to calibrate the moisture measurement function for neutron scattering with zero and another non-zero hydrogen contents because the hydrogen content is linear with the neutron count readings. Once the calibration function for a measurement mode is constructed, we can obtain the calibration table for actual measurements.

During the practical tests, once the nuclear gage is calibrated with the new formulation and procedure, one can use counting number of the neutron scattering for hydrogen content (H) and then use the counting number of the photon (CN) and H to calculate the density. Because the H atoms generally exhibit a small weight in pavement materials, the actual density can be approximated as the density without hydrogen. Therefore, we can use the calibration function to obtain the density immediately.

Because the major improvements are through the fundamental testing principles, the main changes are conducted through the calibration method and count reading analysis. The improved test method will be economically feasible and easy to use as the existing nuclear test method. The team is seeking the opportunity to transfer this technology to industry and demonstrate the method through the field projects. The developed technology together with the new hardware will be released and produce national and international impact on asphalt pavement construction.

To demonstrate this method, we can use the parameters calculated from our measurement data as the calibration function. Then we can re-predict the density from our measurement data. The difference between the prediction and the measurement of density can be used to self-evaluate the consistency of this method.

From the photon reading count number from the different source depths, the density of the mixed sand composites are predicted by Eq. (18) for all the mixed sand composites at BC = 6" (when the radiation source rod was placed 4" from its nearest boundary), which are provided in Figure 25. It shows that there is certain discrepancy between the prediction and the real value when the source depth is 4" from the sample surface. However, when the source depth is relatively at a distance away, say 6" and 8" from the sample surface, the predicted density of the test material based on the presented model agrees very well with the real one for the samples with all the studied moisture contents.
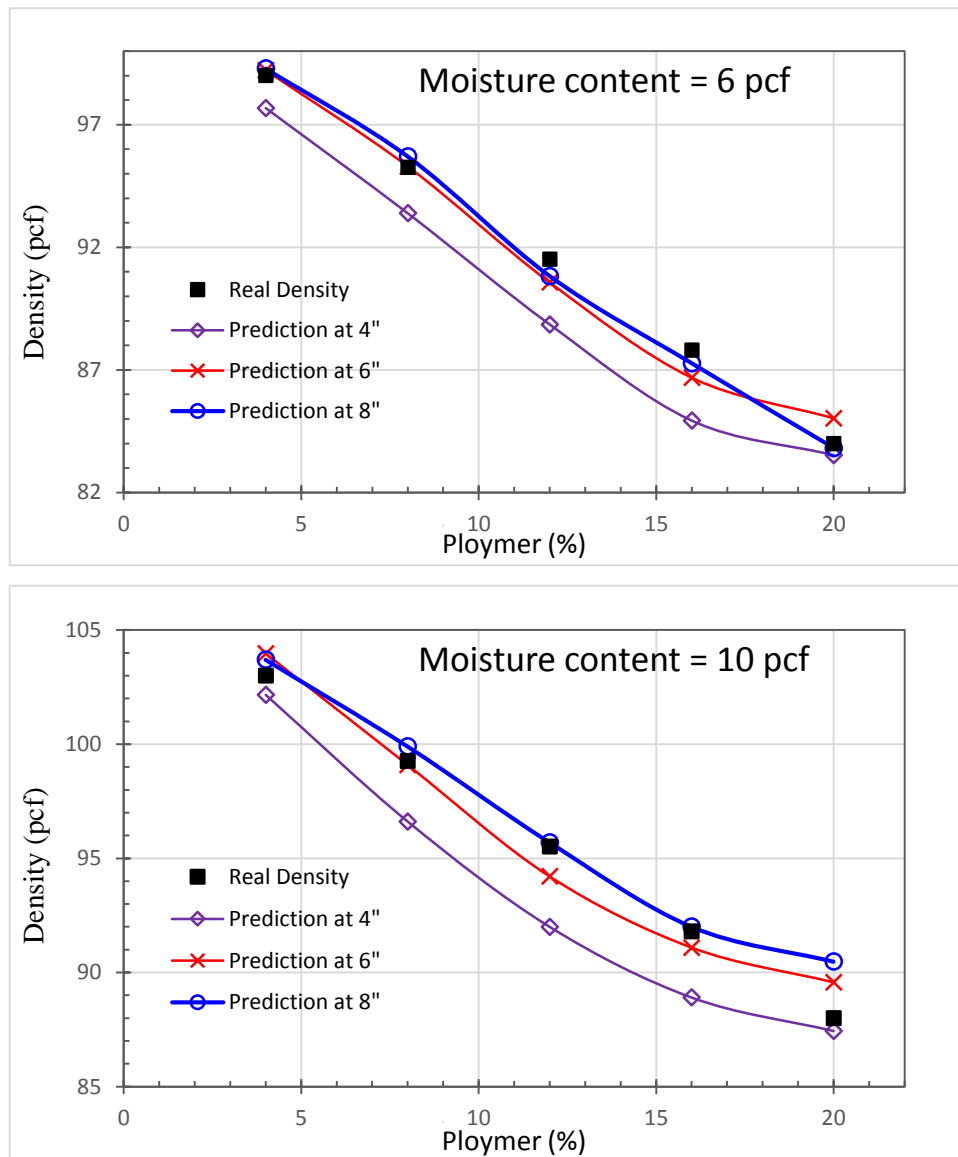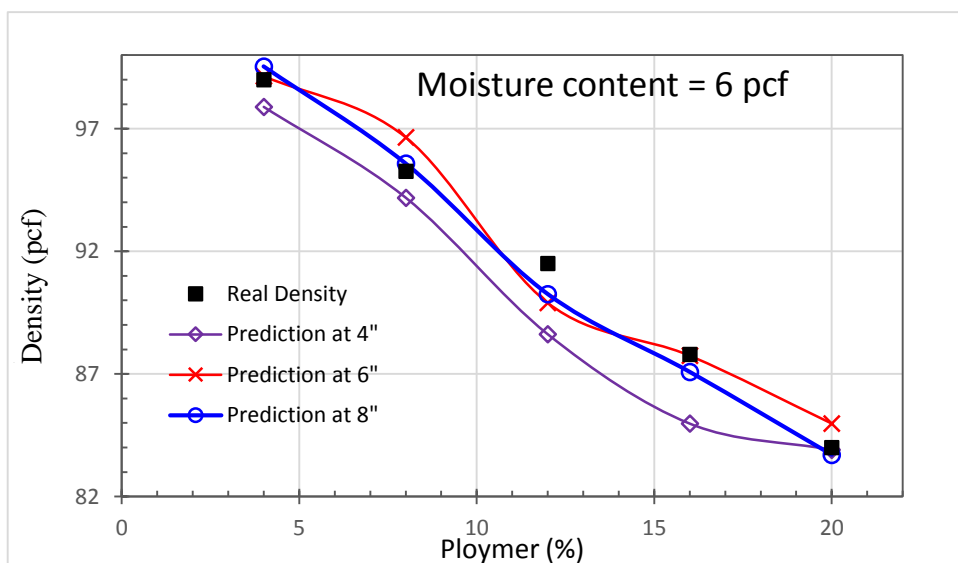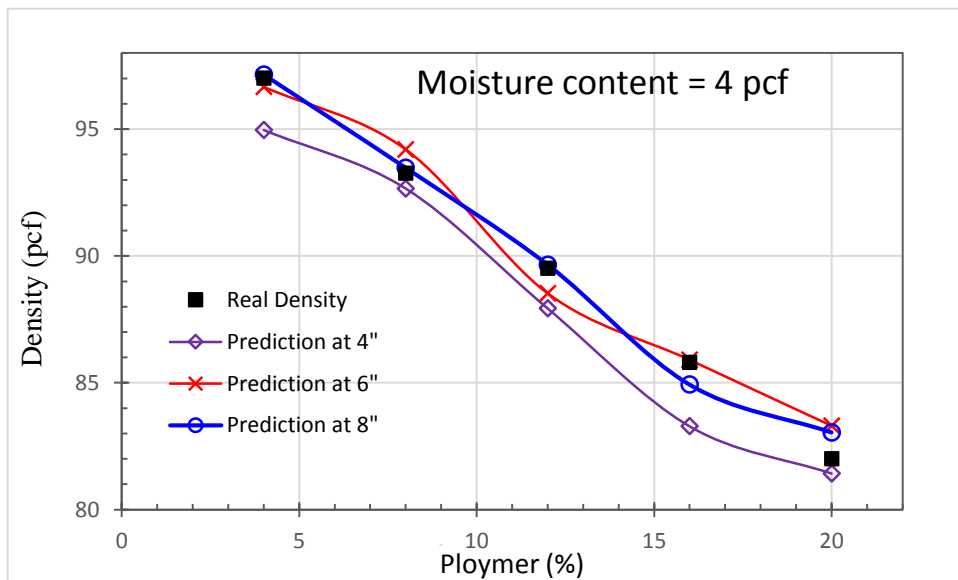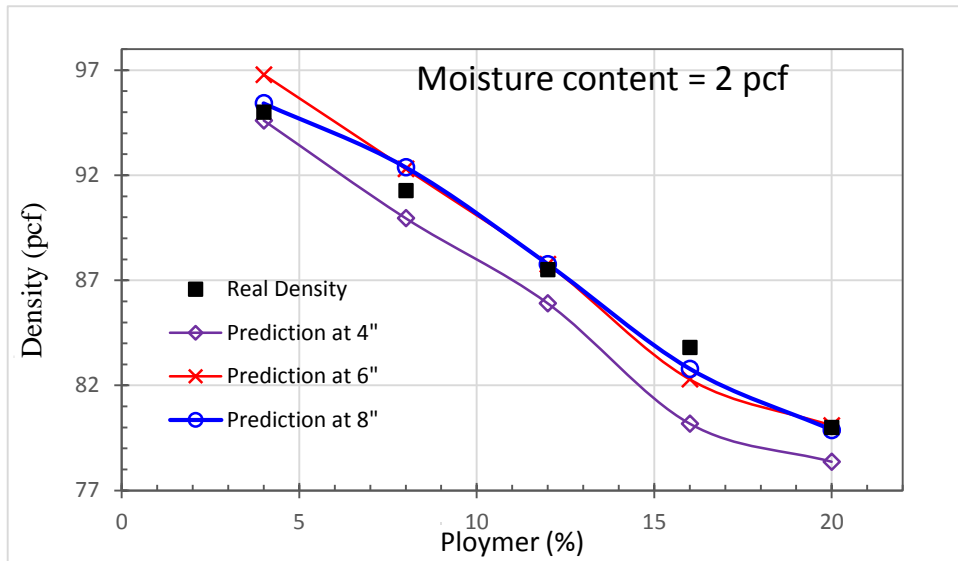
Figure 25. Comparisons of the predicted density by the present model and the real one for samples with different moisture contents at BC = 6 ″.

To further validate the developed model, the photon count numbers of all the mixed sand composites at BC = 4" are applied to predict the sample density. The prediction results are provided in Figure 26, it shows again that the present model underestimates the density of the test samples. However, the predicted densities match well with the real ones for all samples with different moisture contents.
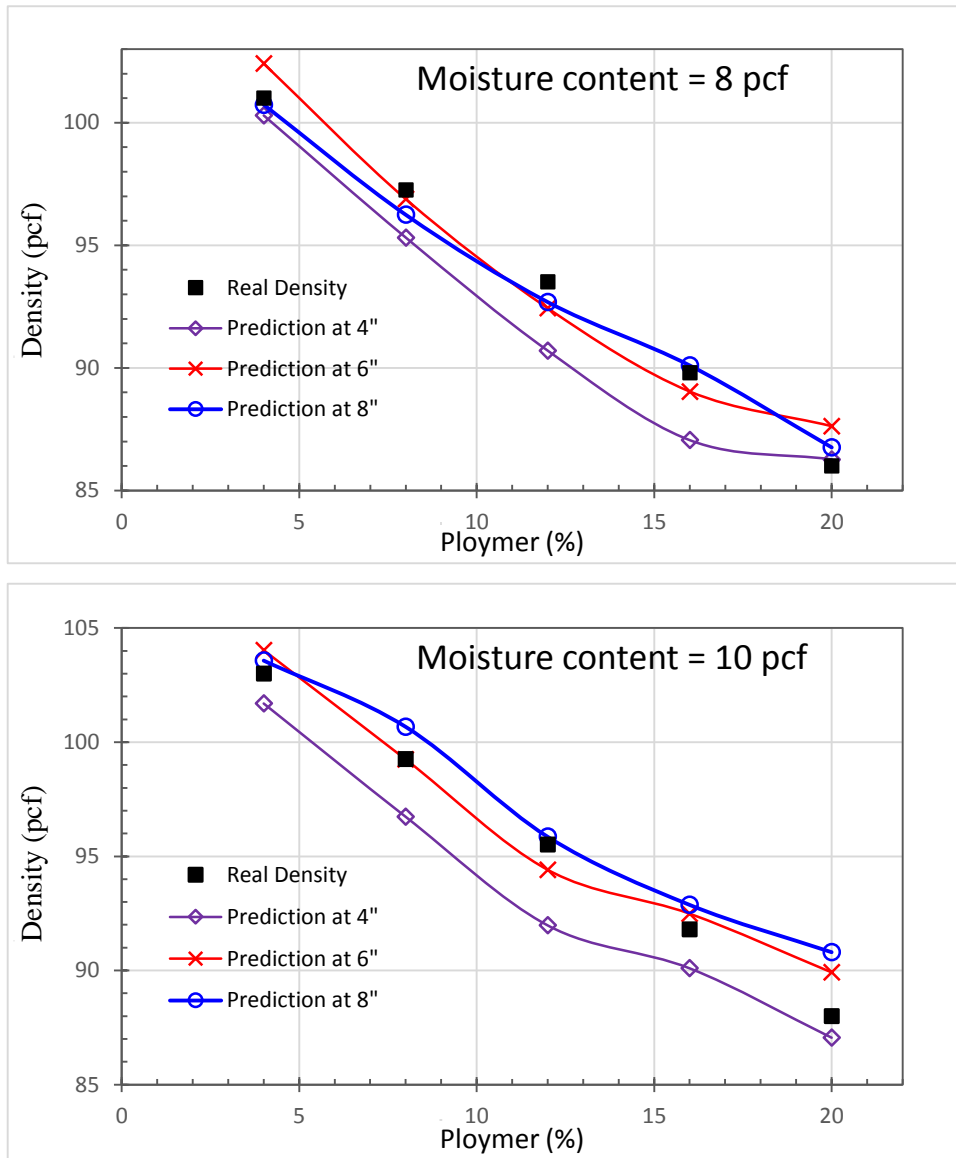
Figure 26. Density comparisons between the prediction by the present model and the real one at BC=4".
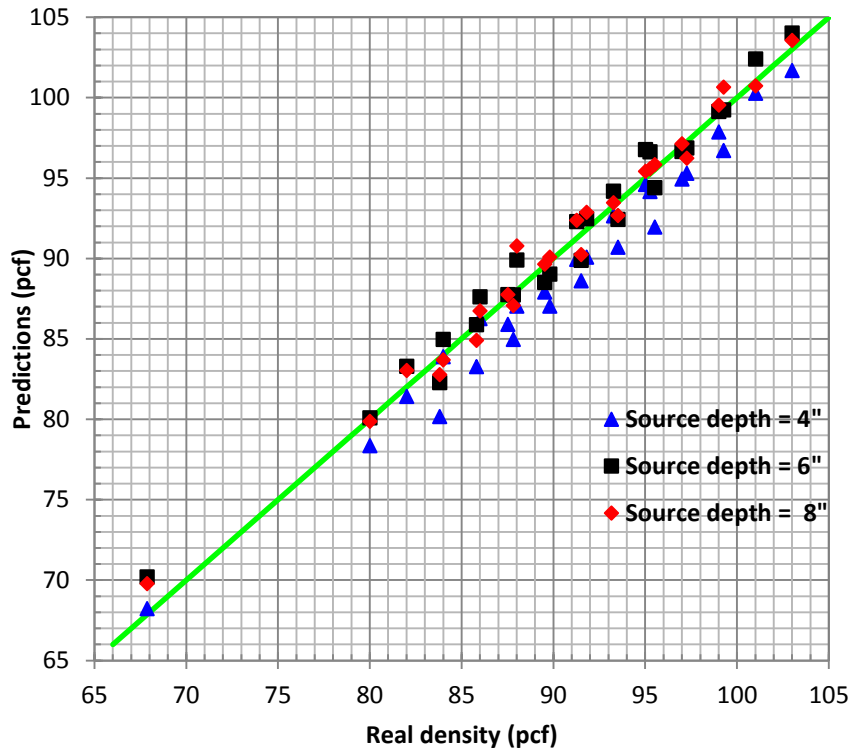
Figure 27. Overall discrepancies between the predicted densities by the decoupled model and the real ones at BC= 4".
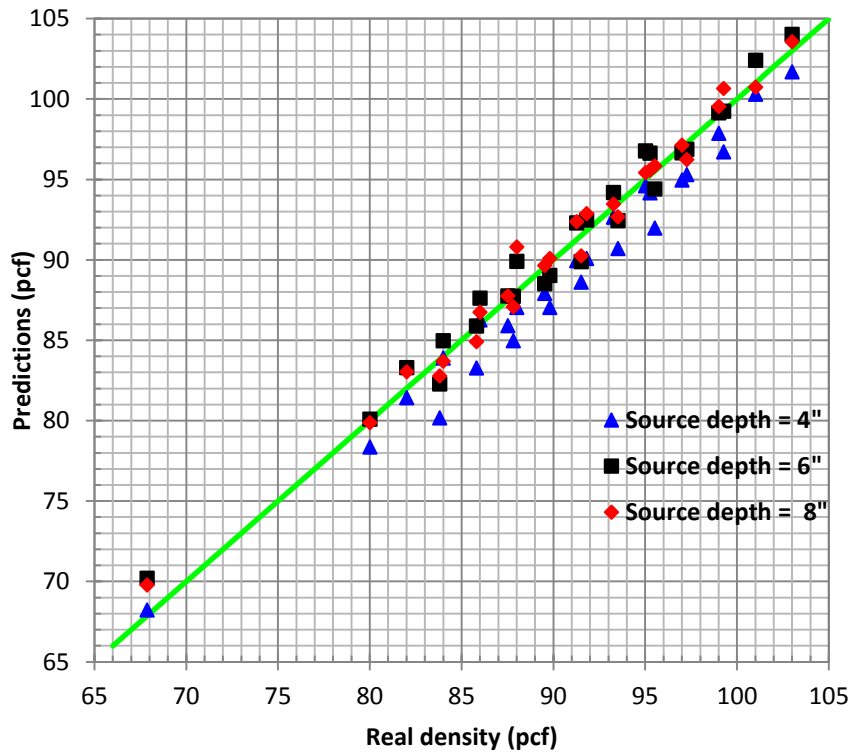

Figure 28. Overall discrepancies between the predicted densities by the decoupled model and the real ones at BC= 6".

The overall discrepancies between the predicted densities by the decoupled model and the real ones for all the tested samples at BC = 4" and BC = 6" are shown in Figure 27 and Figure 28, respectively. While a quantitative assessment of the developed model is presented in Table 11, which provides the coefficient of determination of the predictions and the real densities. Expect the predictions at the 4" (source depth = 4"), the coefficient of determination for the predictions at 6" and 8" are larger than 95%. It demonstrates again that the presented model is able to accurately predict the density of a material with different moisture contents.

It shows from Figure 27, Figure 28 and Table 11 that the all the densities predicted by the presented decoupled model provide a satisfactory assessment for all the samples tested in this study. While the predictions from the count numbers measured at source depths of 6" and 8" agree better with the real ones than that at source depth of 4". It indicates that more reliable density measurements will be obtained by placing the nuclear gauge's source rod into a deeper position to read the count numbers. Notice that a shielding material with certain height is embedded in the nuclear gauge device to protect emission from the radioactive source when the source rod placed in a safety position. As a result, certain amount of photons will be shielded by this shielding material in a measurement when the source rod is placed in a relatively shallow position. It's exciting to notice that this presented model is able to disclose this shielding effect. Thus the present study recommends that the source rod be placed in a relatively deeper position (say h ≥ 6") in order to obtain a reliable measurement.

Table 11 Coefficient of determination (R^2)

Moisture content (pcf)	BC=4"			BC=6"		
	4"	6"	8"	4"	6"	8"
2	85.63	95.29	98.20	81.63	96.62	98.26
4	90.26	97.38	98.62	89.02	98.94	98.62
6	86.65	96.07	98.18	85.24	97.69	99.24
8	85.91	95.36	98.25	80.51	93.81	95.62
10	82.61	95.42	91.85	79.47	95.97	94.95

6.2 Prediction for Asphalt binder and validation

The goal of this project is to improve the accuracy and consistency of the nuclear test methods in asphalt pavement construction through decoupling the attenuation effect of electrons of hydrogen and other types of atoms. To this end, the density of the asphalt binder is predicted through this decoupled model, the real density of the binder prepared in this study is used to compare the predicted one and at the meanwhile to validate this model. The predicted density of the asphalt binder based on the present model is provided in **Error! Reference source not**

found.. Compared to the real density, the predictions based on the present model at different boundary conditions and source depths are about 0.8% to 3.5% higher than the real one, demonstrating that the overall accuracy and consistency of the presented model are acceptable.

Table 12 Density prediction and validation

	BC=	Source depth		
		4″	6″	8″
Predictions (pcf)	4″	68.24	70.21	69.79
	6″	68.41	69.26	69.01
Real density (pcf)		67.86		

7. SUMMARY AND CONCLUSIONS

In this study, the photon absorptions of mixed composites with different density and moisture contents have been investigated using different nuclear sources. The nuclear gauge count reading changing with material density and moisture contents have been characterized and modelled. The correlation between actual block densities and nuclear gauge count readings has been analyzed, through which the effect of the moisture on the density reading gets better understood and the accuracy and consistency of the nuclear test methods are enhanced.

The present study improves the accuracy and consistency of the nuclear test methods in pavement construction through decoupling the attenuation effect of electrons of hydrogen and other types of atoms. A NIST standard mold with fine aggregate mixed with different contents of foam particles and water have been used for nuclear reading in the direct transmission mode. The hydrogen content (H) (and the associated moisture content) has been first measured by neutron scattering. We assume the pure fine aggregate does not contain any hydrogen, which can be used to calibrate the dry density versus the count numbers. Using the count numbers (CN) versus actual density (D) at different hydrogen contents, one can obtain the effects of hydrogen atoms and therefore derive the function of CN in term of D and H in the log scale, which exhibits a linear trend approximately as $\ln(CN) = -k_1 D + k_2 H + b$. Our investigation also disclosed that the effect of the mold boundary can be disregarded as long as the source is beyond 4" to the boundary, but the transmission distance from the source to the detector has significant effect so that the function has different forms for different source depths. Once the photon and neutron count number readings are available, the density of a test material can be uniquely determined by these two readings through the decoupled model: $D = k_1 - k_2 \ln(CN) + k_h CN_{Ne}$. Because of the shielding mechanism configured in the nuclear gauge device, the present study recommends that the source rod be placed in a relatively deeper position (say $h \geq 6$") in order to obtain a reliable measurement.

Based on the discovery of this function of CN related to D and H, we can develop a new calibration method of the nuclear gages with ≥ 3 calibration blocks including one aluminium, one magnesium and one polymer blocks with hydrogen content known. The first two can be used to determine k_1 and b, whereas the last one can be used to determine k_2. Redundant blocks can be used to reduce the accidental errors and improve the accuracy. At the same time, the last two blocks can be used to calibrate the moisture measurement function for neutron scattering. Once the calibration function for a measurement mode is constructed, we can obtain the calibration table for actual measurements.

Because the major improvements are through the fundamental testing principles, the main changes are conducted through the calibration method and count reading analysis. The improved test method will be economically feasible and easy to use as the existing nuclear test method. The team is seeking the opportunity to transfer this technology to industry and demonstrate the method through the field projects. The developed technology together with the

new hardware will be released and produce national and international impact on asphalt pavement construction.
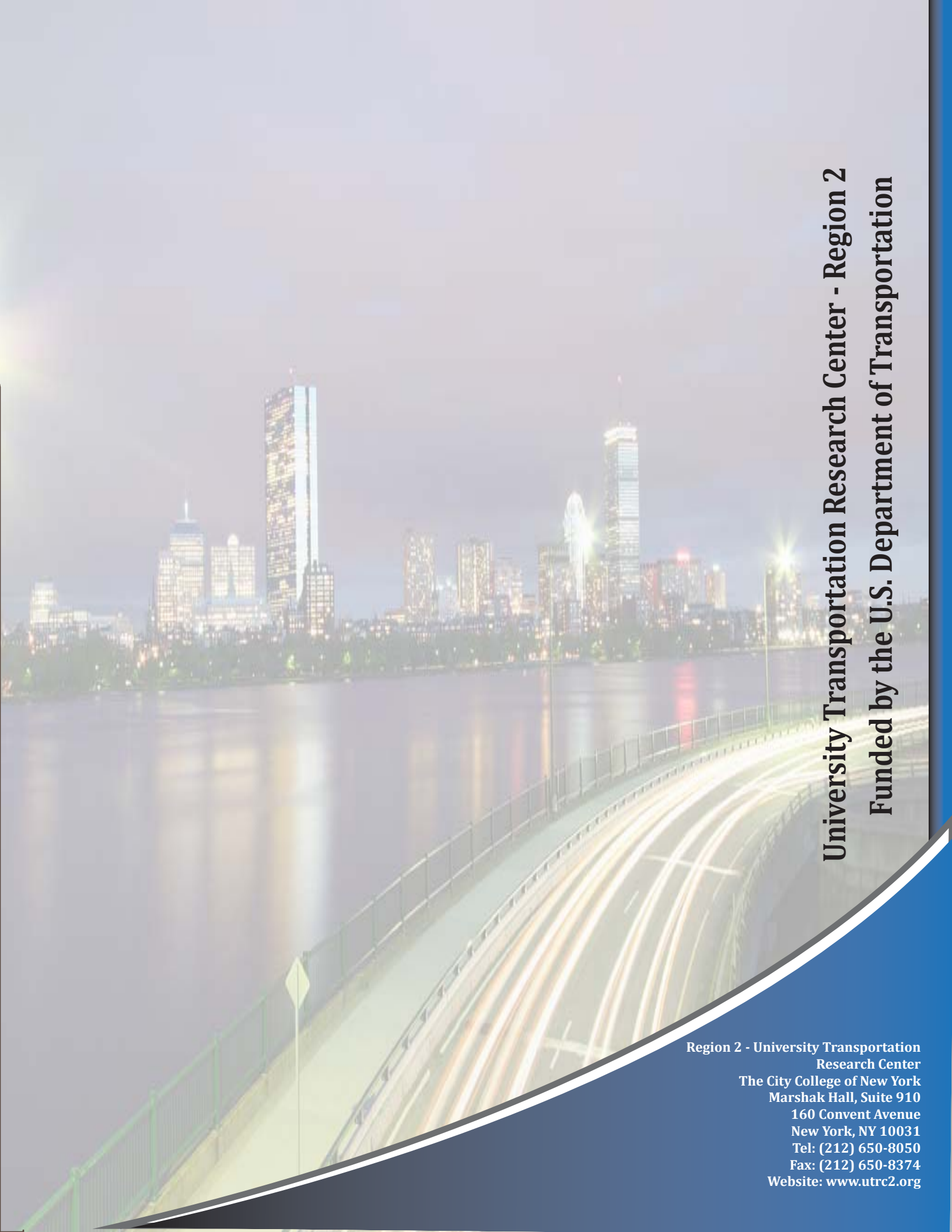
REFERENCES:

[1] Regimand, A., 1999, Validation and calibration apparatus and method for nuclear density gauges, Google Patents.

[2] Yin, H. M., and Luo, Z., 2011, "Investigation of the Nuclear Gauge Density Calibration Method," Road Materials and Pavement Design.

[3] Weber Jr, W. G., 1964, "Laboratory and field evaluation of nuclear surface gages for determining soil moisture and density," Presented at the 43rd Annual Meeting of the Highway Research Board Washington DC January, Washington DC, p. 17.

[4] Hveem, F. N., 1964, Safety manual and administrative instructions to personnel using nuclear probes, California Department of Transportation.

[5] Smith, R. E., and Weber, W. G., 1965, "A BASIC STUDY OF THE NUCLEAR DETERMINATION ON MOISTURE AND DENSITY," California Department of Transportation, Report 225928.

[6] Smith, T. W., Weber, W. G., and Smith, R. E., 1968, Field Evaluation of Compaction Control With Nuclear Gages - Final Report.

[7] Stephens, J., 1964, "Evaluation of nuclear and other device methods for obtaining bituminous paving densities, 6th Annual Paving Conference," 6th Annual Paving Conference, Chicago IL.

[8] LeFevre, E. W., and Manke, P. G., 1968, "A Tentative Calibration Procedure for Nuclear Depth Moisture/Density Gages," Highway Research Record, 248.

[9] Smith, T. W., Shirley, E. C., and Smith, R. E., 1969, Calibration Standards for Nuclear Gages (Density Standards), California Department of Transportation.

[10] Alexander, M. L., and Doty, R. N., 1984, "California study of asphalt concrete density measurement-nuclear versus core density," ASRM STP 829 Placement and Compaction of Asphalt Mixtures.

[11] Burati, J. L., and Elzoghbi, G. B., 1987, "Correlation of nuclear density readings with cores cut from compacted roadways," Transportation Research Record, (1126).

[12] Smith, B., and Diefenderfer, B., 2008, "Comparison of Nuclear and Nonnuclear Pavement Density Testing Devices," Transportation Research Record: Journal of the Transportation Research Board, 2081, pp. 121–129.

[13] Choubane, B., Upshaw, P., Sholar, G., Page, G., and Musselman, J., 2007, "Nuclear Density Readings and Core Densities: A Comparative Study," Transportation Research Record: Journal of the Transportation Research Board.

[14] Padlo, P. T., Mahoney, J., Aultman-Hall, L., and Zinke, S., 2005, "Correlation of Nuclear Density Readings with Cores Cut from Compacted Roadways," Connecticut DOT Report CT-2242-F-05-5.

[15] Minchin, R., Thomas, H., and Swanson, D., 2001, "Theory Behind Vibration-Based, Onboard Asphalt Density Measuring System," Transportation Research Record: Journal of the Transportation Research Board, 1761, pp. 70–78.

[16] Hausman, J., and Buttlar, W., 2002, "Analysis of TransTech Model 300 Pavement Quality Indicator: Laboratory and Field Studies for Determining Asphalt Pavement Density," Transportation Research Record: Journal of the Transportation Research Board, 1813, pp. 191–200.

[17] Prowell, B., and Dudley, M., 2002, "Evaluation of Measurement Techniques for Asphalt Pavement Density and Permeability," Transportation Research Record: Journal of the Transportation Research Board, 1789, pp. 36–45.

[18] Romero, P., and Kuhnow, F., 2002, "Evaluation of New Nonnuclear Pavement Density Gauges with Data from Field Projects," Transportation Research Record: Journal of the Transportation Research Board, 1813, pp. 47–54.

[19] Weber, W. G., 1962, Laboratory Studies of Nuclear Surface Moisture and Density Gages, California Department of Transportation.

[20] Howe, D. R., 1965, Field Use of a Nuclear Soil Gage on Several Concurrent Construction Projects in District 03 and 10, California Department of Transportation.

[21] Howe, D. R., and Lister, B., 1966, Evaluation of the Nuclear Compaction Test Method - District 3, California Department of Transportation.

[22] Howe, D. R., and Lister, B., 1967, Evaluation of the Nuclear Compaction Test Method - District 5, California Department of Transportation.

[23] Gipson, C. T., and Kelly, J. V., 1967, Evaluation of the Nuclear Compaction Test Method - District 02, California Department of Transportation.

[24] Lister, B., Evaluation of the Nuclear Compaction Test Method - District 6, California Department of Transportation.

[25] Lister, B., Evaluation of the Nuclear Compaction Test Method - District 10, California Department of Transportation.

[26] Zube, E., 1967, "Asphalt Concrete Compaction Studies Using Nuclear Devices," University of Pacific, Stockton, California, pp. 1–26.

[27] Castanon, D. R., Chan, E., Chang, J. C., Hannon, J. B., and Forsyth, R. A., 1975, Calibration Standards for Nuclear Gages-Density and Moisture Standards, California Department of Transportation.

[28] 911-c, C. T. M., 1974, Method of Developing Density and Moisture Calibration Tables for the Nuclear Gauge.

[29] 111, C. T. M., 2005, Method of Developing Density and Moisture Calibration Tables for the Nuclear Gauge.

[30] Obermuller, J. C., Smith, T. W., Hirsch, A. D., and Hatano, M., 1971, Relative Compaction Study, California Department of Transportation.

[31] Chan, E. E., Champion, F. D., Chang, J. C., Hannon, J. B., and Forsyth, R. A., 1975, "IMPROVED PERFORMANCE CRITERIA FOR USE IN NUCLEAR GAGE SPECIFICATIONS."

[32] Lister, B., and Baumeister, K. L., 1975, Testing of Thin Layers With Nuclear Gages, California Department of Transportation.

[33] Scrimsher, T., 1977, Study of Vacuum Extractor- Vacuum Pycnometer and Nuclear Procedures for Determining Asphalt Content in Asphalt Concrete, California Department of Transportation.

[34] Chan, E. L., 1976, Improved Nuclear Gage Development-Phase 1 & 2, California Department of Transportation.

[35] Zha, J., 2000, Revisions of California Test Method 111 for Nuclear Gauge Calibration.

[36] "Ionization" [Online]. Available: https://www.nde-ed.org/EducationResources/CommunityCollege/Radiography/Physics/Ionization.htm. [Accessed: 18-Jul-2015].

[37] "Introduction to Radiation - Introduction-to-Radiation-eng.pdf."

[38] "Sources of Attenuation" [Online]. Available: https://www.nde-ed.org/EducationResources/CommunityCollege/Radiography/Physics/attenuation.htm. [Accessed: 18-Jul-2015].

[39] US Department of Commerce, N., "NIST: X-Ray Mass Attenuation Coefficients" [Online]. Available: http://www.nist.gov/pml/data/xraycoef/. [Accessed: 29-Jul-2015].

University Transportation Research Center - Region 2

Funded by the U.S. Department of Transportation